Synthesis, characterization, antioxidant and anticancer human studies of new metal ion complexes of poly Schiff base derived from 4-aminoacetophenone with 4-chloroaniline and salicylaldehyde

Mohammed HA Al-amery* and Tamara QM al-sahlanee
Department of Chemistry, College of Sciences, University of Baghdad, Baghdad, IRAQ
*dr.al_amery1954@yahoo.com

Abstract
New metal ion complexes of some transition metal ions [Cu(II), Cr(III), Fe(III), VO(II) and Co(II)] of prepared ligand 2-(((4-(1-((4- chlorophenyl) imino)ethyl) phenyl) imino) methyl) phenol were synthesized. The ligand was prepared by Schiff base procedure which included the reaction of p-chloroaniline with 4-aminoacetophenone with salicylaldehyde and the structures of the new metal ion complexes were characterized by Elemental Micro Analysis (C.H.N), FT-IR, UV-Vis spectra, Thermal Gravimetric Analysis (TGA-DTG), Flame Atomic Absorption, Molar Conductivity, Magnetic Susceptibility measurement and Mass Spectra.

According to the obtained data, the probable coordination geometries of these complexes were suggested as octahedral except C_4 as pyramidal. All complexes were found to be non-electrolyte. The anticancer activity was screened against Human brain cancer cells (AMJM), Cervical cancer cells (HeLa), Ovarian cancer cells (SKOV-3) and Breast cancer cells (MCF-7). The results indicate that the metal ion complexes show increased cytotoxicity in proliferation to cell lines as compared to free ligand.

Keywords: Anticancer, Transition metal ions, Schiff base.

Introduction

In the second half of the last century, the coordination chemistry gained a large area of chemistry for its rapid development in the practical aspect of the preparation of complexes as well as their contribution to the knowledge of the structures of these complexes. These complexes have played an important and increasing role in industry[1], agriculture[2] and medicine[3]. The formation of metal complexes is a general phenomenon which is not confined only to the transition elements[4], but to the represented elements[5] observed especially in the transition elements providing empty orbitals. Schiff bases are important organic ligands to coordinate with metal ions[6]. Schiff bases have been known since 1864. Schiff base or Schiffs base is a type of chemical compound containing a carbon-nitrogen double bond as functional group. Schiff bases are generally prepared by condensation of primary amines ($-NH_2$) with active carbonyl compounds like aldehydes and ketones (>C=O). They are also known as anils, imines and azomethine[8].

Schiff bases are considered as a very important class of organic compounds having wide applications in many biological aspects. Moreover, some Schiff bases and their metal complexes exhibit antibiotic, antitumor, anticancer, anti-inflammatory, antifungal, corrosion inhibition, antibacterial, antimalarial, antiviral activity and anti-HIV[9]. The Schiff bases are relatively stable, but Schiff bases derived from aromatic compounds are more stable than those derived from aliphatic compounds. The aliphatic aldehydes are relatively unstable and readily polymerize while those of aromatic aldehydes are having effective conjugation which are more stable. Cell culture is one of the major tools used in cellular and molecular biology, providing excellent model systems for studying the normal physiology and biochemistry of cells (e.g. metabolic studies, aging), the effects of drugs, toxic compounds on the cells, a mutagenesis and carcinogenesis. It is also used in drug screening and development and large-scale manufacturing of biological compounds (e.g. vaccines, therapeutic proteins).

The major advantage of using cell culture for any of these applications is the consistency and reproducibility of results that can be obtained from using a batch of clonal cells. Human cancer cell line cultures are considered to be a model of physiological functioning in vivo; so these enable research on cancer cell biology and are useful for developing new strategies to prevent cancer cell growth and progression of the disease.

Material and Methods

The chemicals (organic, inorganic and solvent): The chemicals used included 4-chloroaniline (Sigma-Aldrich), 4-aminoacetophenone (Sigma-Aldrich), Salicyladehyde (Sigma-Aldrich), $CuCl_2.2H_2O$ (Merck), $CrCl_3.6H_2O$ (BDH), $FeCl_3$ (BDH), $VOSO_4.5H_2O$ (BDH) and $CoCl_2.6H_2O$ (Merck). The organic solvents which were used included ethanol 95% (BDH), dimethylsulfoxide (DMSO) (LOBA cheme) and petroleum ether (30-60ºC) (Fluka).

Maintenance of cell cultures (anticancer activity): Cell lines were obtained from the Iraq Biotech Cell Bank Unit and maintained in RPMI-1640 supplemented with 10% Fetal bovine, 100 units/mL penicillin and 100 µg/mL streptomycin. Cells were passaged using Trypsin-EDTA

reseeded at 50% confluence twice a week and incubated at 37 °C.

Synthesis of Ligand

Step 1: 4-aminoacetophenone (1mmole), (0.13gm) was dissolved in absolute ethanol (15mL), then three drops of glacial acetic acid were added and 4-chloro aniline (1mmol), (0.12gm) was added to the solution of 4-aminoacetophenone. The mixture was heated under reflux at temperature 70°C for ten hrs. During this period, a yellow solid compound was formed which was collected by washing with ethanol to remove unreacted materials and dried in oven under 70°C giving yellow crystals as shown in the following equation (1):

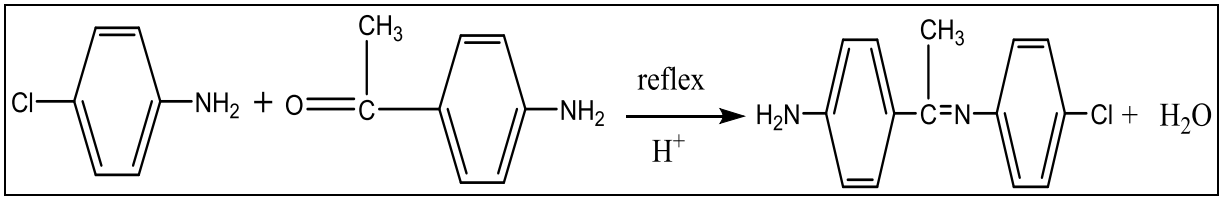

Equation 1: Synthesis of 4-(1-(4-chlorophenyl)imino)ethyl)aniline

Step 2: Mix (1mmole), (0.24gm) from the derivative recorded above with 10mL, 0.12gm from salicylaldehyde in (50mL) ethanol absolute. The mixture was heated under reflux at temperature 70 °C for eight hrs. and then let the mixture cool until the precipitate. The solid precipitate was filtered, washed by absolute ethanol and dried to get the ligand pure as shown in in the following equation 2:

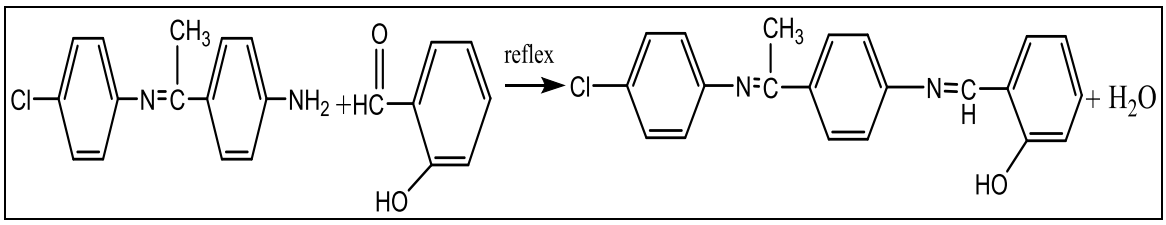

Equation 2: Synthesis of ligand

Synthesis of Complexes: A solution of (0.697gm, 0.001mol) of the ligand (L) in 8mL of absolute ethanol was added drop wise to warm solution (0.001mol) of metal salts (0.34gm, (0.532gm, 0.324gm, 0.506gm and 0.474gm for $CuCl_2.2H_2O$, $CrCl_3.6H_2O$, $FeCl_3$, $VOSO_4.5H_2O$ and $CoCl_2.6H_2O$ respectively) dissolved in 10 ml absolute ethanol and the mixture was refluxed for 4-8 hrs. Colored crystalline solid compounds were formed. The products were filtered, washed with ethanol and dried in oven.

Cytotoxicity Assays: To determine the cytotoxic effect, the MTT cell viability assay was done using 96-well plates. Cell lines were seeded at 1 X 10^4cells/well. After 24 hr., a confluent monolayer was achieved. Cells were treated with tested compound. Cell viability was measured after 72 hrs. of treatment by removing the medium, adding 28 µL of 2 mg/mL solution of MTT (and incubating the cells for 1.5 h. at 37 °C. After removing the MTT solution, the crystals remaining in the wells were solubilized by the addition of 130 µL of DMSO (Dimethyl Sulphoxide) followed by 37 °C incubation for 15 min with shaking [10]. The absorbency was determined on a microplate reader at 492 nm (test wavelength); the assay was performed in triplicate. The inhibition rate of cell growth (the percentage of cytotoxicity) was calculated as follows:

Inhibition rate = A-B/A *100

where A and B are the optical density of control and the optical density of test.

Antioxidant activity:

DPPH radicals scavenging assay: Antioxidant activity (x-substance) was measured using stable radicals with minor adjustments[11]. X-substance was used to investigate the scavenging activity. The samples were mixed with 450 µL of DPPH solution and then complete the volume of mixture to one ml using absolute ethanol. Ascorbic acid was used as a positive control at concentration 10 µg/mL. The samples and control are left in dark at room temperature for 30 minute. The absorbance was measured at 517 nm.

Results and Discussion

Microanalysis: The importance of preparing Schiff base compounds arises from its versatility as starting material for the synthesis of many compounds. The structures of the prepared Schiff base with its metal ion complexes were identified by C.H.N (Table 1), FT-IR (Table 2), UV-Visible (Table 3), ^{1}H-NMR (Table 4), ^{13}C-NMR (Table 5) and TGA-DTG (Table 6) with some other techniques.

FT-IR Spectral Studies: Important characteristic stretching frequencies of the ligand and its metal ion complexes are described in table 2 and their spectra are shown in figures 1-6. 2-(((4-(1-((4- chlorophenyl) imino)ethyl) phenyl) imino) methyl) phenol (L) as a bidentate ligand normally coordinates with metal ions through nitrogen of the azomethine group and OH of salicylaldyde[12]. The bands related to υ(C=N) stretching vibration of the free ligand (L)

appeared at (1566) cm^{-1} [13]. The band related to OH vibration appeared at range (3200-3500) cm^{-1} [14]. The bands related to υ(C=N) stretching vibrations of the complexes were shifted to 1533, 1537, 1535, 1541 and 1537 cm^{-1} respectively of the complexes (C_1, C_2, C_3, C_4 and C_5) as a result of coordination with metal ions through the lone pair electrons of nitrogen atom. The band at (1236) cm^{-1} which was assigned to the δ(C-O) group of (L) was shifted in the spectra of complexes (C_1-C_5) to (1242, 1257, 1245, 1253 and 1242) cm^{-1} respectively.

The peaks which appeared at (370, 351, 352 and 385) cm^{-1} respectively of complexes (C_1-C_3 and C_5) were attributed to υ M-Cl, while peaks at (487, 489, 491, 491 and 457) cm^{-1} respectively of complexes refer to υ M-O, while peaks at (518, 536, 592, 599 and 501) cm^{-1} respectively of complexes refer to υ M-N, that supports the complexes formation[15]. The spectrum of the complex C_4 showed sharp medium band at (975) cm^{-1} assigned to stretching vibration of ν(V=O)[16] and two bands appeared at (370-440) cm^{-1} and (340-410) cm^{-1}, which were assigned to the anti-symmetrical and symmetrical vibrations respectively of the stretching V-S[17].

Molar Conductance Measurement: The molar conductance values of the synthetic complexes obtained in DMSO as a solvent at room temperature were listed in table 3. The results which are given in this table showed that all complexes have non-electrolytic nature[18].

Electronic Spectra (UV-Visible) Studies: The UV-Visible spectrum of the ligand (L) showed intense band at 31347 cm^{-1} which belonged to $\pi \rightarrow \pi*$ as shown in figure 7. The electronic spectra of the ligand and its metal ion complexes were recorded for their solution in DMSO at room temperature (10^{-4} M). The electronic spectrum of the (C_1) complex showed one (d-d) transition observed at 19607 cm^{-1} may be assigned to the transition $^2Eg \rightarrow {}^2T_2g$ [19]. Magnetic moment value 1.87 B.M is in accordance with those having distorted octahedral. The spectrum of the complex (C_2) showed three bands observed at (11123, 19841 and 20920) cm^{-1}; these bands may be assigned to the transitions $^4A_2g \rightarrow {}^4T_2g$, $^4A_2g \rightarrow {}^4T_1g(F)$ and $^4A_2g \rightarrow {}^4T_1g(p)$ respectively. The value of magnetic moment was (4.02) B.M.

The spectrum of the complex (C_3) showed two bands observed at (19493 and 27777) cm^{-1}. The first band may be assigned to the transition $^6A_1g \rightarrow {}^4T_2g$ and the second band may be assigned to the charge transition. The magnetic moment value was 5.72 B.M. The spectrum of the complex (C_4) showed two bands observed at (10204 and 19569) cm^{-1}; these bands may be assigned to the transitions ($^2B_2g \rightarrow {}^2Eg$) and ($^2B_2g \rightarrow {}^2A_1g$) respectively. The magnetic moment value was (1.74) B.M. The spectrum of the C_5 showed three bands observed at (14771, 15822 and 16694) cm^{-1} respectively; these bands may be assigned to the transitions (^4T_1g (F) → ^4T_2g (F)), (^4T_1g (F) → ^4E_2g (F)) and (^4T_1g (F) → ^4A_2g (P)) respectively. The magnetic moment value was 4.5 B.M.

^{1}H-NMR/and ^{13}C-NMR Spectra: The ligand was characterized by ^{1}H-NMR and ^{13}C-NMR spectroscopic methods, in addition of all complexes using DMSO d^6 as a solvent. The ^{1}H-NMR spectrum of the ligand (L) showed five peaks; the first peak appeared at δ(~2.5) ppm which was assigned to the solvent peak (DMSO), the second peak which appeared at δ(1.81) ppm was assigned to the (CH_3) proton, the third peak which appeared at δ(8.62) ppm was assigned to the (C=NH) proton while the fourth peak appeared at δ(11.57) ppm which corresponded to the (OH) of salicylaldehyde. The last peak appeared at (6.67-8.04) ppm attributed to the aromatic protons[20].

^{1}H-NMR spectra of the complexes were different to that of the ligand. The signal of (C=NH) of the ligand was shifted in these complexes to (9.98, 10.14, 9.38, 8.98 and 9.37) ppm for (C_1-C_5) respectively and the signal of (OH) was shifted in these complexes to (12.80, 12.00, 12.51, 12.24 and 12.09) ppm for (C_1-C_5) respectively while the signal of (CH_3) shifted to range (1.99-1.51) ppm. The new peak appeared in (3.51-3.78) ppm refers to protons of water molecule in the complexes (C_1, C_2, C_4 and C_5). Another peak was shown in the complex (C_3) appeared at (1.07, 3.40 and 3.47) ppm referring to proton CH_3, CH_2 and OH of ethanol solvent respectively[21], this gave an indication for complexes formation. The ^{1}HNMR spectra results were listed in table 4 and shown in figures 13-18.

The ^{13}C-NMR spectrum of the ligand showed peaks; the first one appeared at (~40) ppm and corresponded to the solvent peak (DMSO), while the second peak appeared at (169) ppm and corresponded to the (N=C-CH_3) carbon while the third peak appeared at (165.7) ppm which corresponded to the (N=CH) carbon atom. The other peak appeared at (143.94 and 155.95) which corresponded to (C-N) carbons.

The spectrum appearance at low fields at δ = (151) ppm was assigned to (C-O) of salicylaldehyde. The chemical shift of (C-aromatic ring) appeared at = (112.11-138.33) ppm. while chemical shift of (CH_3) appeared at = (15.1) ppm [20]. The ^{13}C-NMR spectra of the complexes (C_1-C_5) showed difference peaks: the signal of (N=CH) carbon of the ligand was shifted in these complexes to (166, 167, 167, 165 and 168) ppm for (C_1-C_5) respectively. The signal of (C-N) carbon was shifted in these complexes to (147, 144, 144, 148 and 145) ppm respectively and the signal of (C-O) of salicylaldehyde were shifted to range (152-154) ppm. Other peaks were shown in the complex (C_3) appearing at 18.36 and 56.16 ppm to proton CH_3 and CH_2 of ethanol solvent respectively. The ^{13}C-NMR spectra results were listed in table 5 and shown in figures 19-24.

Thermal analysis of the ligand and their metal ion complexes: Thermal analysis TG and DTG of complexes was studied under nitrogen gas at heating range (25-600)°C

and heating rate(10ºC/min).The thermal analysis was performed to proof the suggested structures. The results were listed in table 6 and shown in figures 25-30.

Mass Spectra: Mass spectrometry has been successfully used to investigate molecular species in solution[22]. The Schiff base (L) and its complexes were compared with their molecular formula weight. The mass spectra of ligand and its complexes were shown molecular ion peak at m/z = (349, 600, 613, 556, 602 and 587) for the ligand and its complexes respectively. These data are in good agreement with the proposed molecular formula for ligand and complexes. It also shows series of some peaks corresponding to various fragments. The intensities of these peaks give the idea of the stabilities of the fragments (Supplementary material). Mass spectra were shown in figures 31-36.

Cytotoxicity Assays (anticancer activity): The toxicity of many anticancer agents is partially due to the inability to distinguish between normal and tumor cells. We selected compound for their primary anticancer assay[23]. In order to eliminate toxicity, it is necessary to identify some specific properties of cancer cells different from normal cells[24], numerous transition metal complexes have been synthesized and screened for their anticancer properties[25]. In order to study action of ligands and complexes to cancer cells, first measure the anti-proliferation activity of these ligands and complexes by the MTT assay. It was found that most compounds in most concentrations have the ability to kill human brain cancer cells, cervical[26] cancer cells, ovarian cancer cells and breast cancer cells in a concentration-dependent manner.

Schiff base ligand improves the anticancer properties of the complex[27]. The increase in the percentage of cell inhibition may be due to the presence of Schiff base[28], but the mechanics are unknown, another suggestion to kill cancer cells is that Schiff base azomethine linkage (–C=N) is an essential structural requirement for biological activities including antibacterial, antifungal and antitumor activities[29,30].

Antioxidant Activity: Antioxidant activity of ligand (L) and its complexes was measured using stable DPPH radicals with minor adjustments. DPPH (2,2-diphenyl-1-picryl-hydrazyl) radical scavenging activity (RSA) evaluation is a standard assay in antioxidant activity studies and offers a rapid technique for screening the radical scavenging activity of specific compounds or extracts[31]. DPPH is a stable free radical that can accept an electron or hydrogen radical and get converted to a stable, diamagnetic molecule. DPPH has an odd electron and so has a strong absorption band at 517 nm.

When this electron becomes paired off, the absorption decreases stoichiometrically with respect to the number of electrons or hydrogen atoms taken up. Such a change in the absorbance by this reaction has been extensively adopted to test the capacity of several molecules to act as free radical scavengers. Hence, more rapidly is the absorbance decrease, the more potent is the antioxidant activity of the compound. The free radical scavenging effects of all the compounds with the DPPH radical were evaluated under the same condition[32].

DPPH radical scavenging activity: Percentage activity of solutions of ligands (L_1 and L_2) and their complexes was studied and compared. Initially free ligand showed negligible DPPH activity, however upon linked with metal ions (Cu, Cr, Fe, VO and Co), the activity was enhanced significantly. All the metal complexes showed comparable or slight less activity to that of standard (ascorbic acid). All the metal complexes showed much better activity than the ligand. The copper complex showed pronounced reducing power than the other metal complexes[32].

Table 1
Elemental, micro analysis and some physical properties of the ligand and the prepared complexes

Comp.	M.Wt. g.mol^{-1}	Yield %	Color	M.P (°C)	Micro elemental analysis Calc. (Found)			M % Cal (Found)	Cl % Cal (Found)
					C%	H%	N%		
L	348.5	72	Yellow	78-80	72.30 (71.12)	4.87 (4.80)	8.03 (7.87)	-----	10.18 (10.65)
C_1	519.44	70	Dark-Brown	122-124	48.55 (47.98)	4.04 (4.06)	5.39 5.65)	12.24 (11.99)	20.51 (20.47)
C_2	614.99	67	Green	110-112	40.97 (41.22)	4.71 (4.69)	4.55 (4.52)	8.45 (8.32)	23.08 (22.75)
C_3	556.84	88	Blak	106-108	49.56 (49.44)	4.13 (4.12)	5.02 (5.35)	10.02 (10.00)	25.50 (27.47)
C_4	601.44	82	Light green	185-187	41.89 (42.00)	4.48 (4.67)	4.65 (4.29)	8.46 -----	5.90 (5.32)
C_5	586.43	71	Pink	90-92	42.97 (42.58)	4.94 (4.90)	4.77 (5.13)	10.04 (10.01)	18.16 (18.23)

Table 2
FT-IR spectra of the ligand (L) and the metal ion complexes

Comp.	υ (OH), H_2O coordination	υ (C=N)	υ (C-O)	υ (M-N)	υ (M-O)	υ (M-Cl)
L_1	3394	1236		-----	-----	-----
C_1	3450	1533	1242	518	487	370
C_2	3465	1537	1257	536	489	351
C_3	3413	1535	1245	592	491	352
C_4	3444	1541	1253	599	491	-----
C_5	3407	1537	1242	501	457	385

Table 3
Electronic spectra, spectra parameter and magnetic susceptibility, molar conductance and suggested stereo chemical of the ligand and the metal ion complexes

Comp.	Wavelength λ(nm)	Wave no. $\bar{\upsilon}$ (cm^{-1})	Assignment	Molar Cond. $S.cm^2\ moL^{-1}$	μeff. (B.M)	Geometry Suggested
L	319	31347	π →π*	…….	……	……
C_1	510	19607	$^2Eg \rightarrow {}^2T_2g$	1.51	1.87	Distorter octahedral
C_2	899 504 478	11123 19841 20920	$^4A_2g \rightarrow {}^4T_2g$ $^4A_2g \rightarrow {}^4T_1g(F)$ $^4A_2g \rightarrow {}^4T_1g(P)$	2.54	4.02	Octahedral
C_3	513 360	19493 27777	$^6A_1g \rightarrow T_2g$ C.T	4.40	5.72	Octahedral
C_4	980 511	10204 19569	$^2B_2g \rightarrow {}^2Eg$ $^2B_2g \rightarrow {}^2A_1g$	2.39	1.74	pyramidal
C_5	677 632 599	14771 15822 16694	$^4T_1g(F) \rightarrow {}^4T_2g(F)$ $^4T_1g(F) \rightarrow {}^4E_2g(F)$ $^4T_1g(F) \rightarrow {}^4A_2g(F)$	2.11	4.5	Octahedral

Table 4
^{1}H-NMR data of the ligand (L) and the metal ion complexes

Comp.	O-H	N=CH	C-H aromatic	H_2O	CH_3 proton
L	11.57	8.62	6.67-8.04	-----	1.81
C_1	12.80	9.98	6.74-7.91	3.74	1.99
C_2	12.00	10.14	6.31-8.03	3.51	1.72
C_3	12.51	9.38	6.93-8.19	-----	1.51
C_4	12.24	8.98	6.55-8.09	3.78	1.91
C_5	12.09	9.37	6.37-8.03	3.65	1.60

Table 5
^{13}C-NMR data of ligands (L) and some of the metal ion complexes

Comp.	HC=N	C-O	C-N	C-H aromatic	CH_3 proton
L	165.7	151.8	143.9	112.1-138.3	15.1
C_1	166.55	152.61	147.52	115.8-139.81	15.62
C_2	167.43	154.23	144.83	111.72-137.93	16.33
C_3	167.40	154.26	144.43	113.19-137.90	15.99
C_4	165.47	153.14	148.09	109.02-138.52	15.26
C_5	168.78	154.03	145.14	114.20-138.50	16.19

Table 6
Thermal decomposition data of the ligand and complexes

Comp.	Molecular formula	Step	Temp. range of the Decomposition C°	Suggested Formula of loss	Mass loss% Cal.	Found
L	$C_{21}H_{17}N_2OCl$ 348.5	1 2 3	60-170 171-380 380-595 > 600	CH_3 $C_6H_4Cl,2C_6H_4$ C,CH Residue (OH,2N)	4.30 75.60 7.17 12.91	3.99 75.59 6.91 13.51
C_1	$[Cu(L_1)Cl_2.2H_2O]$ 519.046	1	100-595 > 600	$2H_2O,2Cl,C_6H_4CH_3$ Residue ($CuC_6H_4CHNC_6H_4CNCl$)	38.14 62.33	37.82 62.18
C_2	$[Cr(L_1)Cl_3.H_2O]5H_2O$ 614.99	1 2	75-379 380-595 > 600	$6H_2O,2Cl$ ClC_6H_4,OH, CH_3, Cl Residue ($CrC_6H_5CHNC_6H_4CN$)	29.10 29.10 41.95	29.11 28.86 42.03
C_3	$[Fe(L_1)Cl_3.C_2H_5OH]$ 556.84	1 2	120-249 250-595 595-600 > 600	CH_3CH_2OH C_6H_4Cl,Cl OH,Cl Residue ($FeClC_6H_4CHNC_6H_4C(CH_3)N$)	8.26 26.39 9.42 55.91	8.88 25.92 9.87 55.81
C_4	$[VO(L_1)SO_4.H_2O]4H_2O$ 601.44	1 2 3	100-279 280-457 458-494 > 600	$4H_2O$ $H_2OC_6H_4$ $ClCH_3$ Residue ($VOSO_4OHCHNC_6H_4CNC_6H_4$)	11.97 15.62 8.39 64.00	11.95 15.85 7.95 64.24
C_5	$[Co(L_1)Cl_22H_2O]4H_2O$ 586.43	1 2	225-388 389-594 > 600	$6H_2O$ C_6H_4Cl Residue ($Co,2Cl,OHC_6H_4CHNC_6H_4C(CH_3)N$)	18.41 19.01 62.57	19.01 19.11 61.88

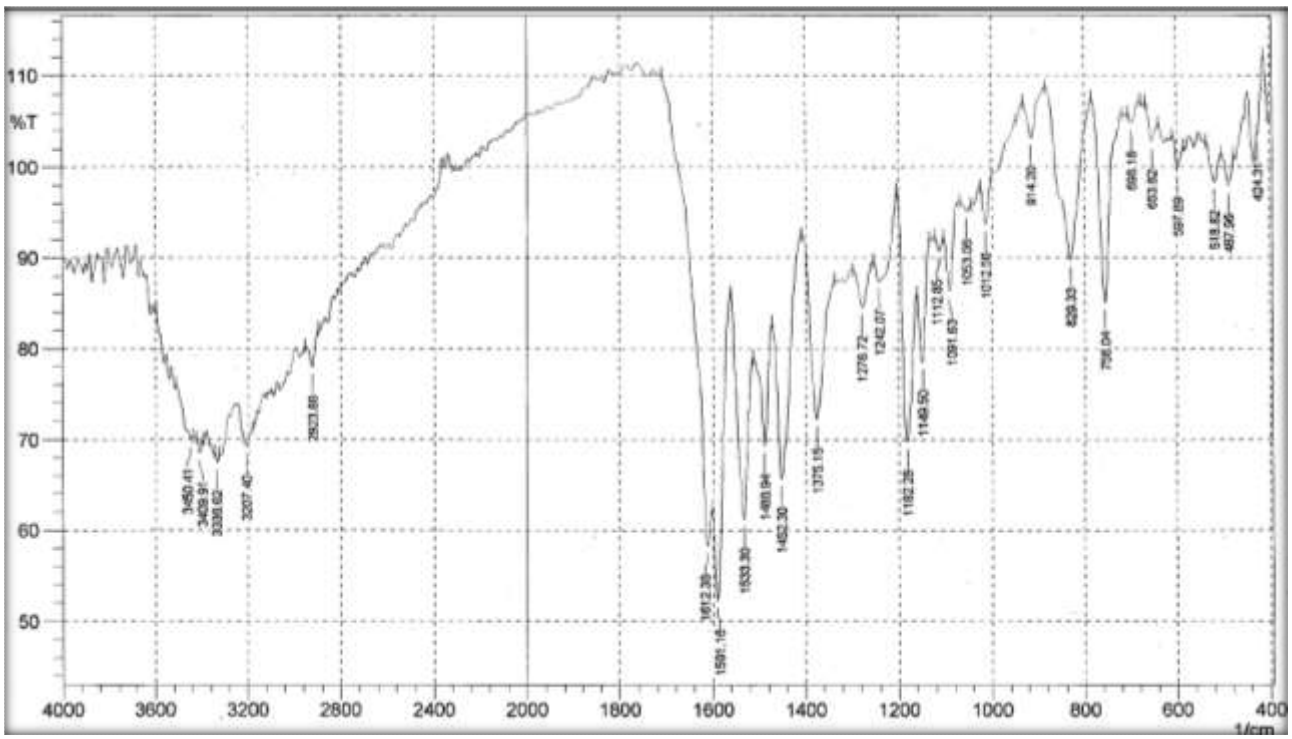

Figure 1: FT-IR spectrum of ligand

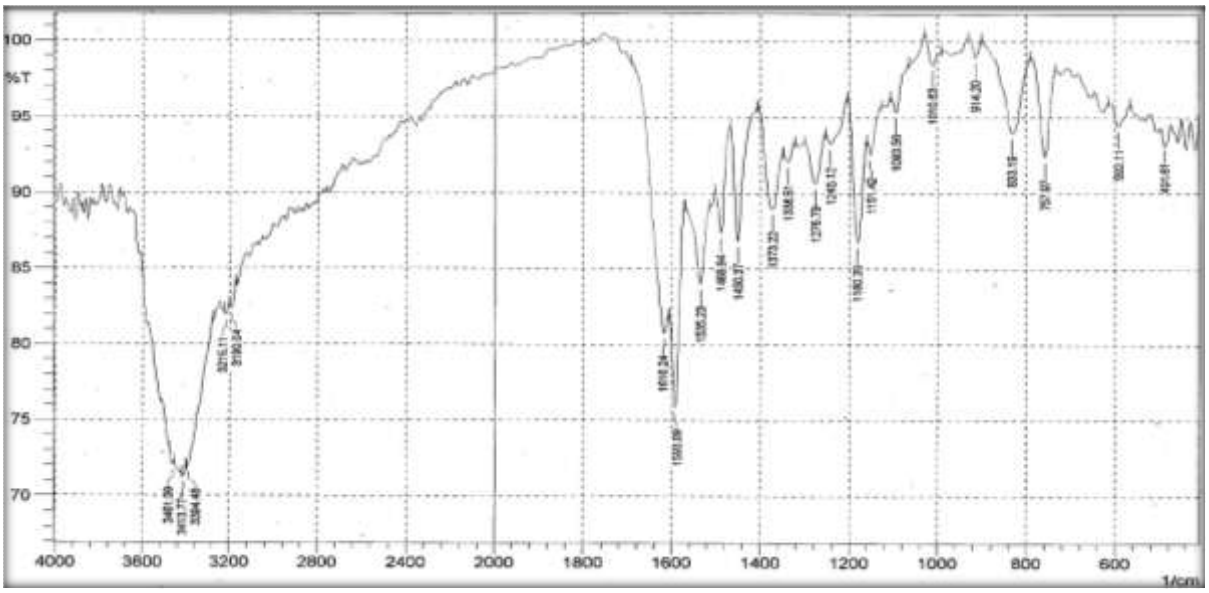

Figure 2: FT-IR spectrum of C_1 complex

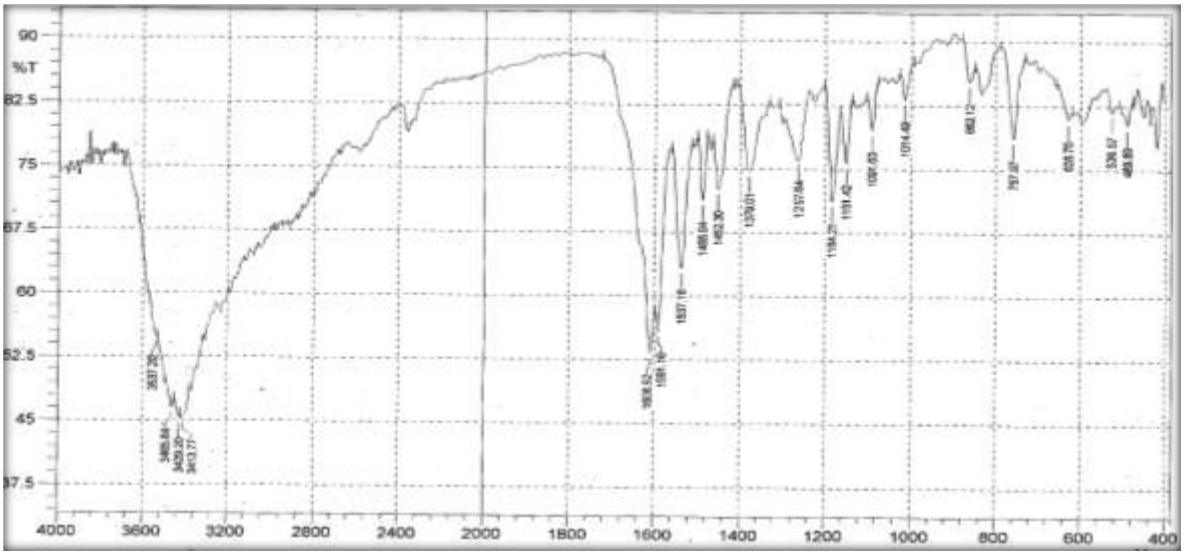

Figure 3: FT-IR spectrum of C_2 complex

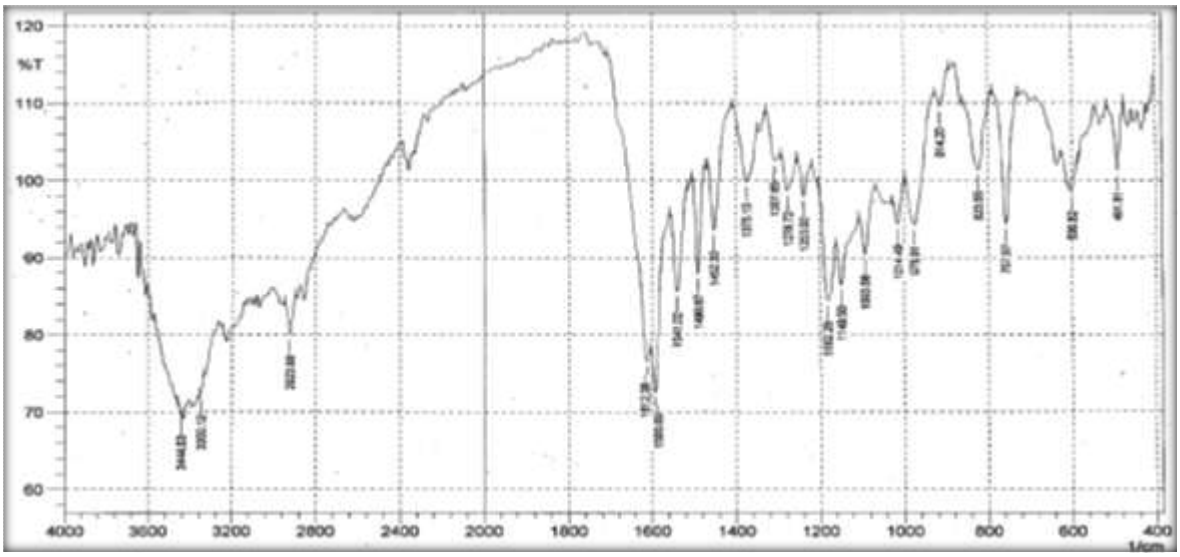

Figure 4: FT-IR spectrum of C_3 complex

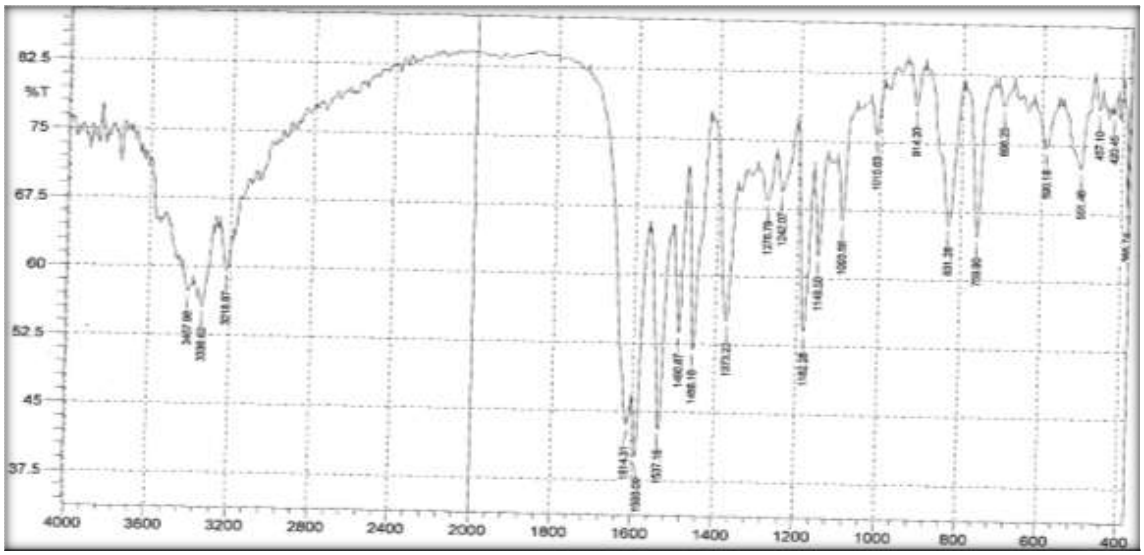

Figure 5: FT-IR spectrum of C_4 complex

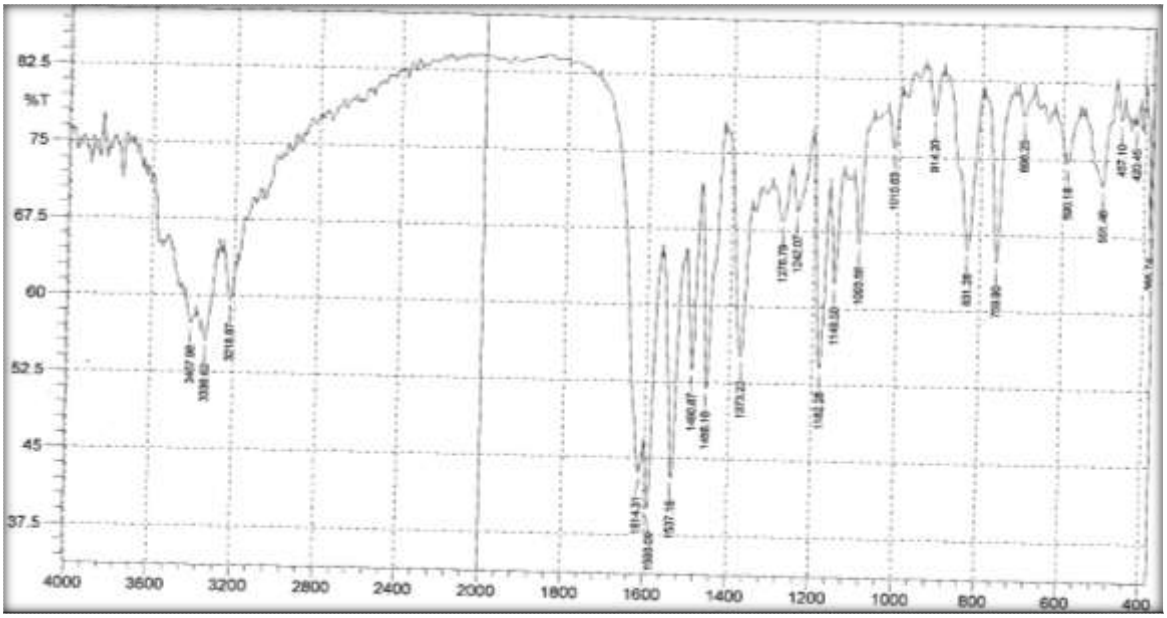

Figure 6: FT-IR spectrum of C_5 complex

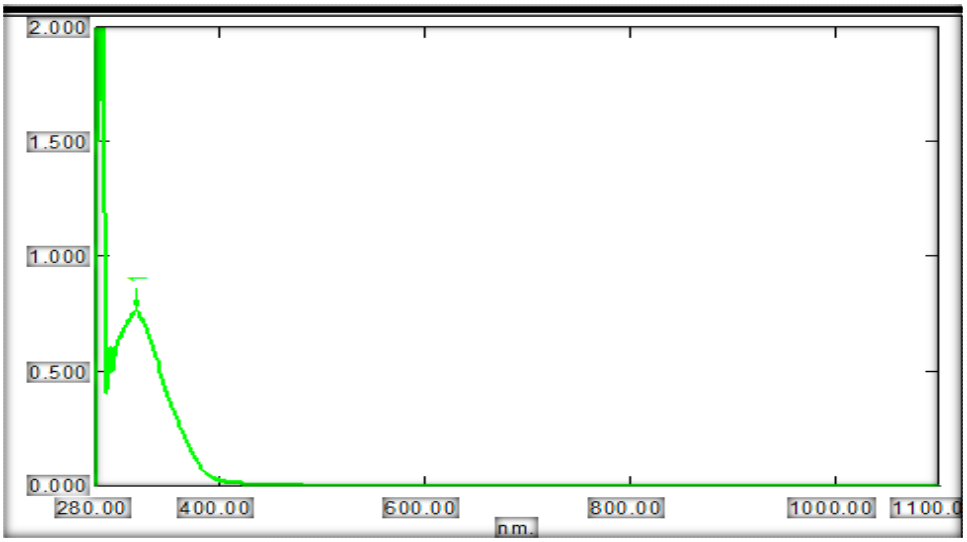

Figure 7: UV-Vis spectrum of L

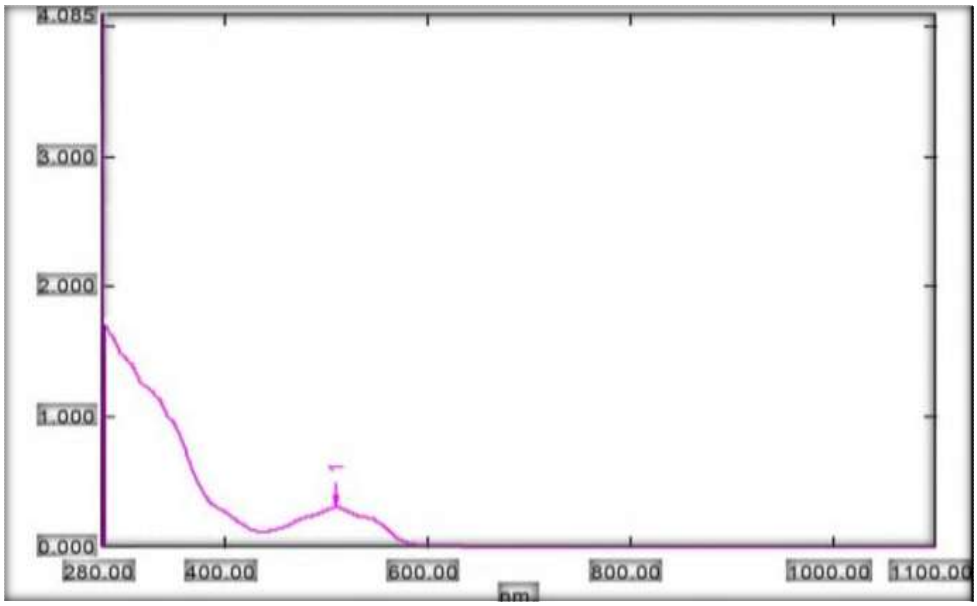

Figure 8: UV-Vis spectrum of C_1 complex

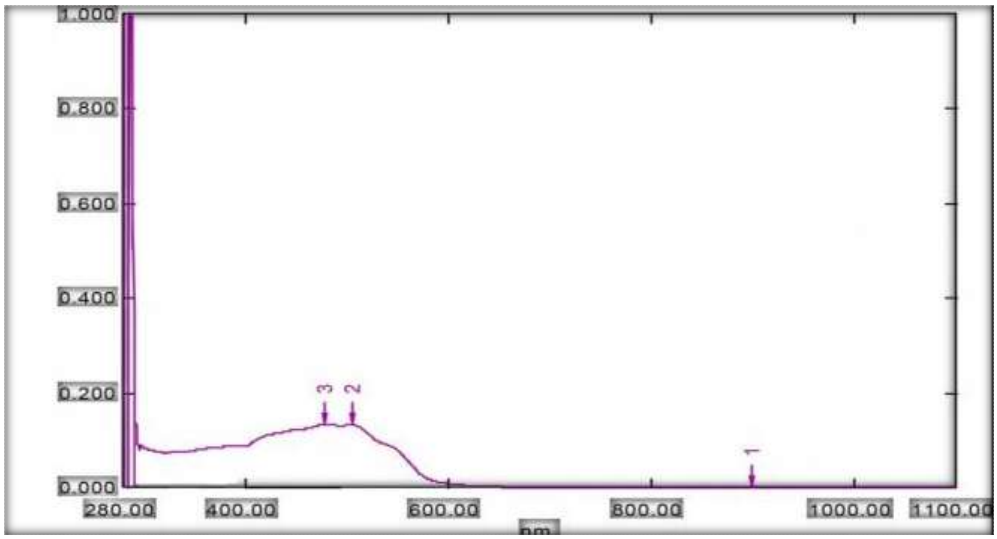

Figure 9: UV-Vis spectrum of C_2 complex

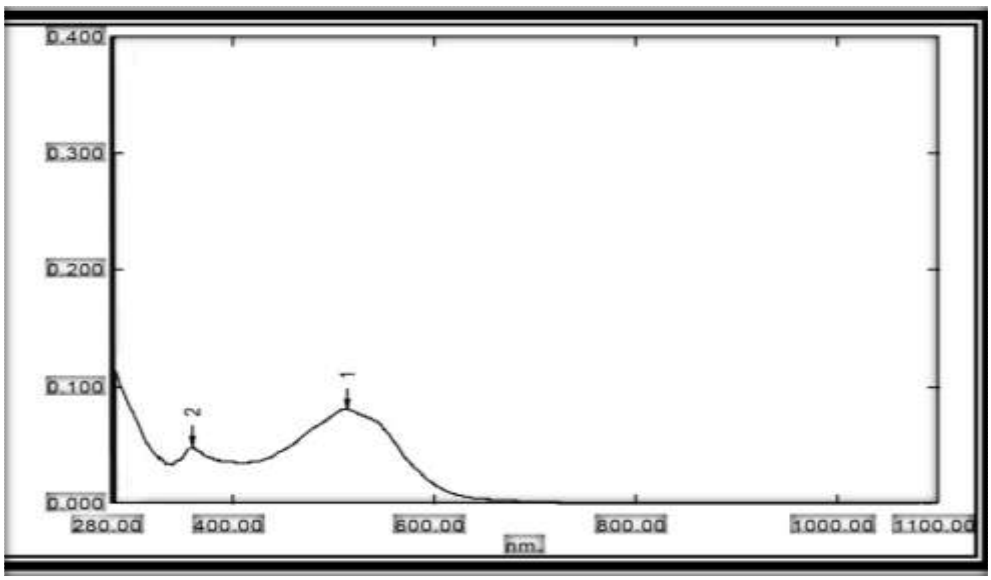

Figure 10: UV-Vis spectrum of C_3 complex

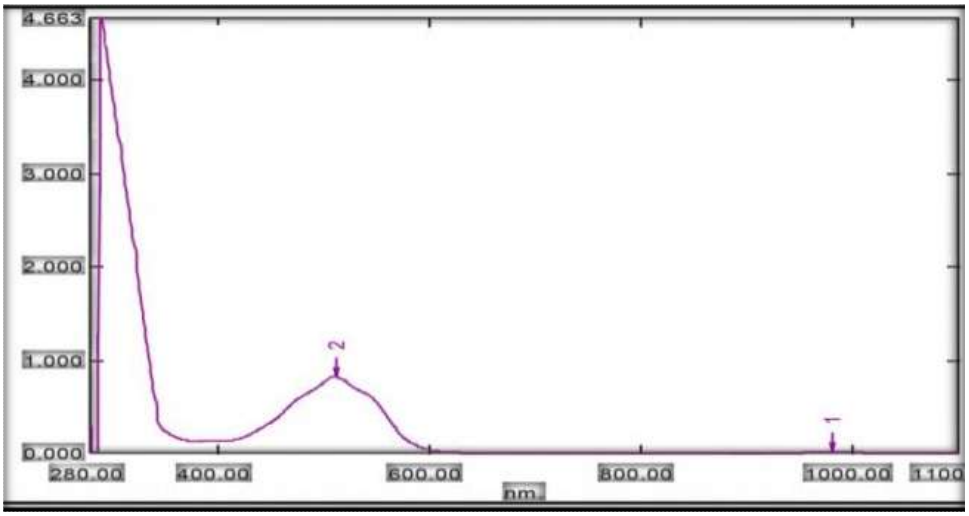

Figure 11: UV-Vis spectrum of C_4 complex

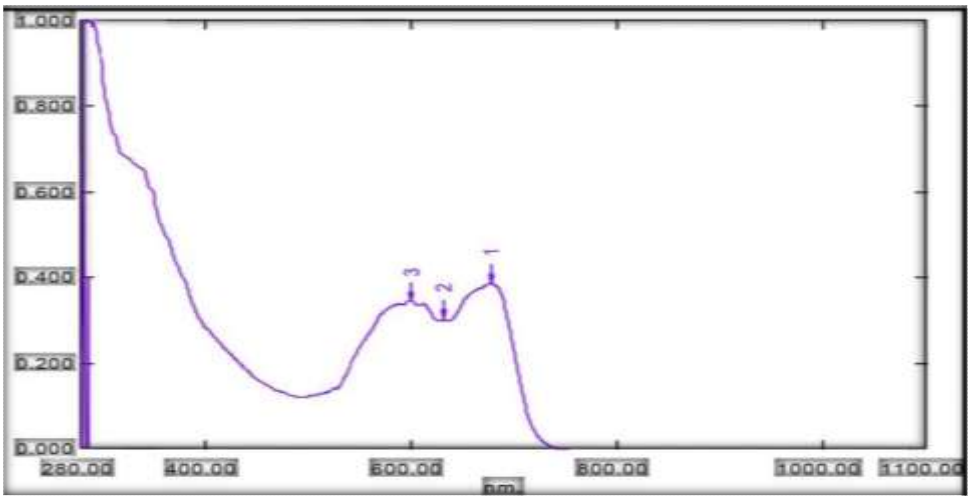

Figure 12: UV-Vis spectrum of C_5 complex

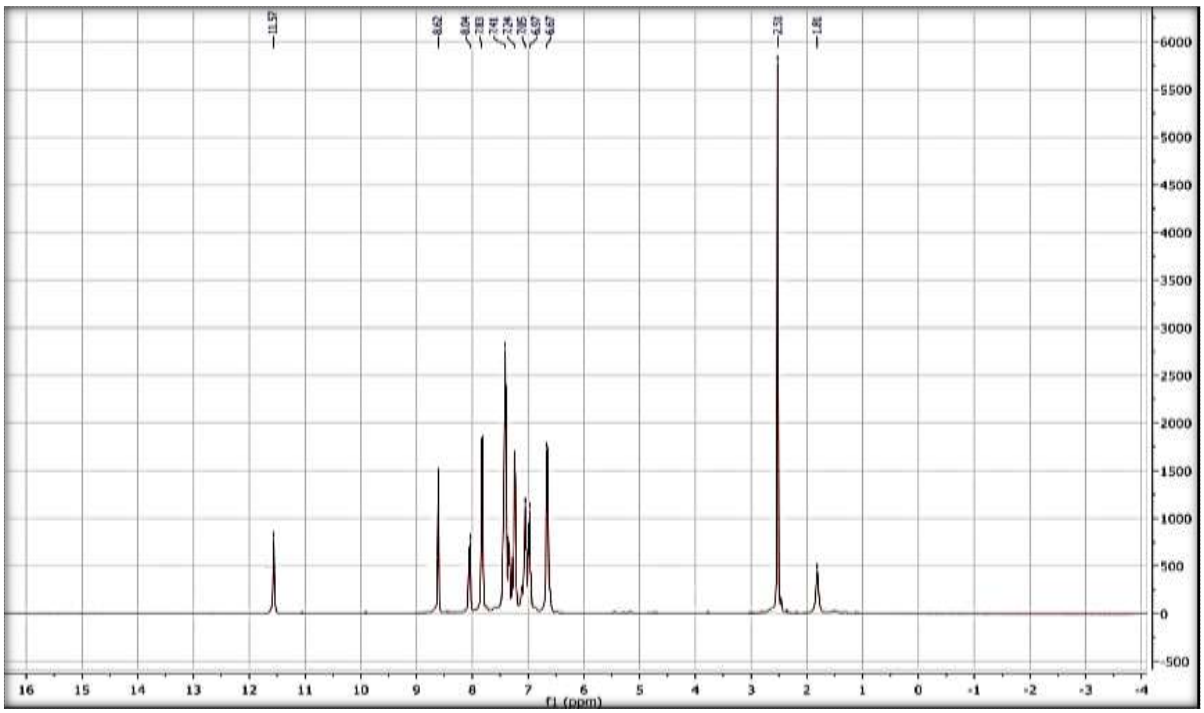

Figure 13: ^{1}H-NMR Spectrum of L

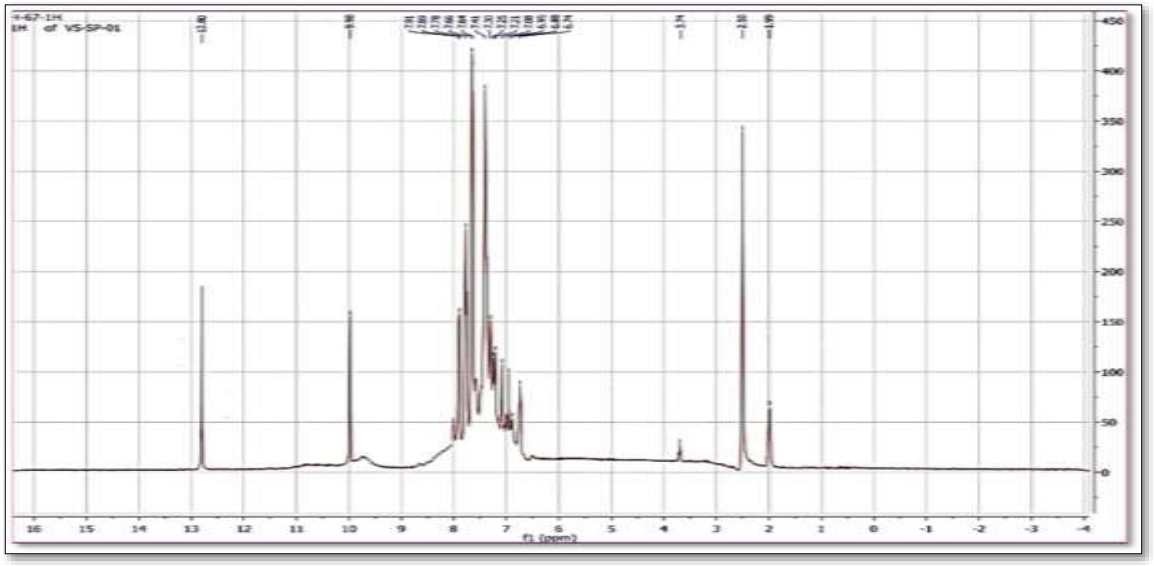

Figure 14: ^{1}H-NMR Spectrum of C_1 Complex

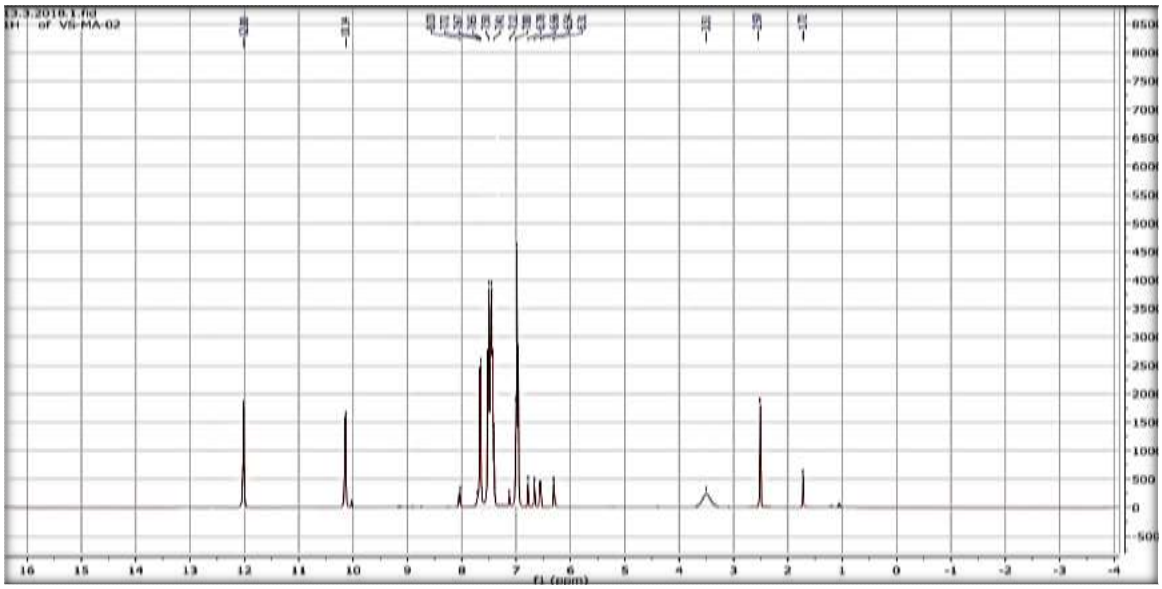

Figure 15: ^{1}H-NMR Spectrum of C_2 Complex

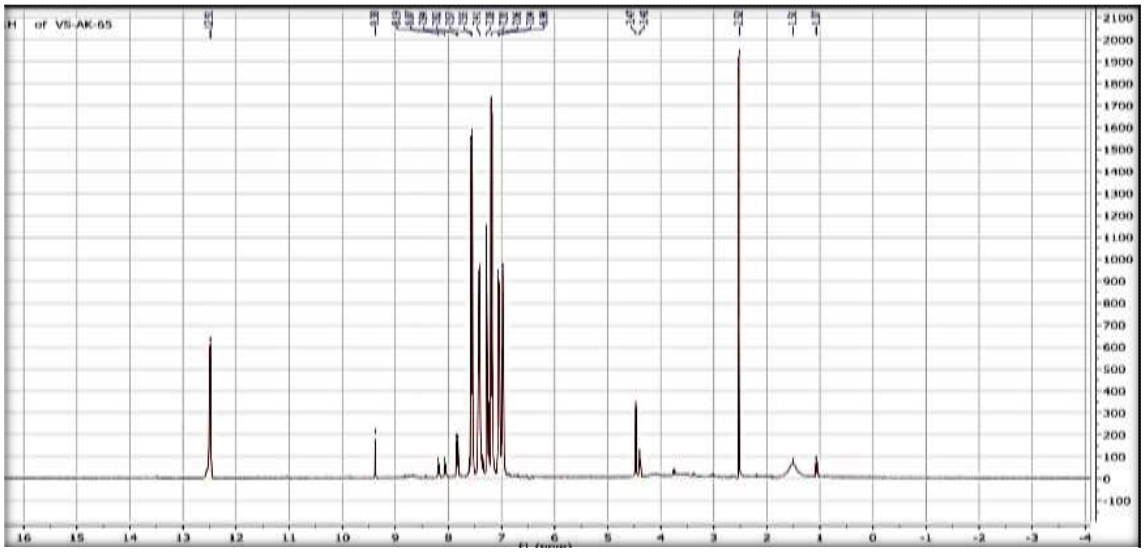

Figure 16: ^{1}H-NMR Spectrum of C_3 Complex

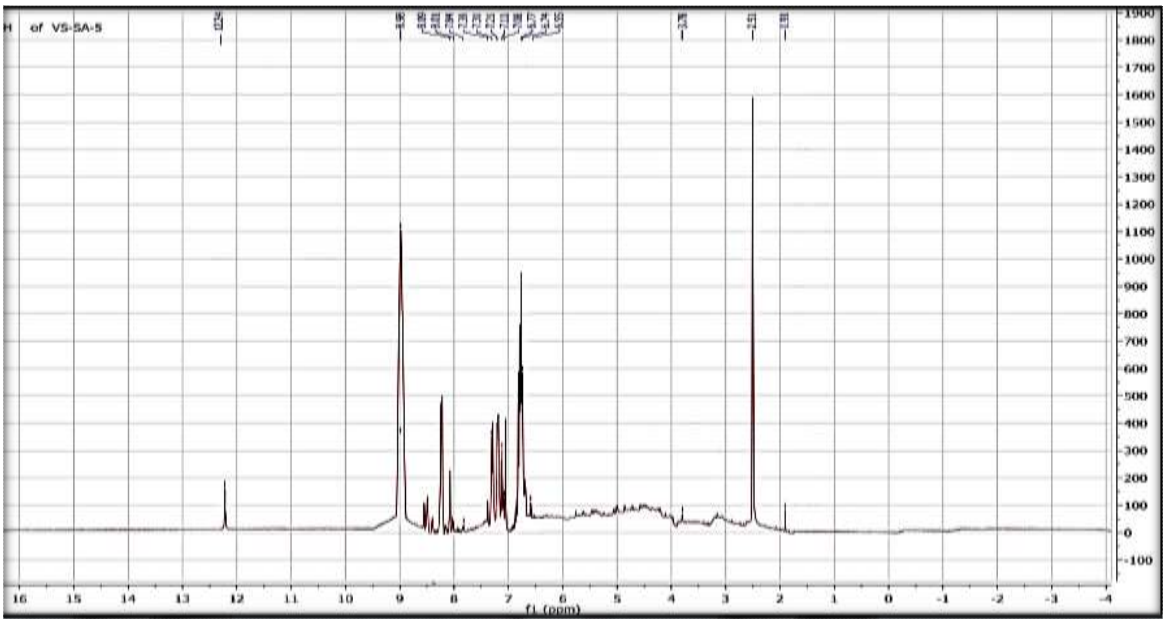

Figure 17: ^{1}H-NMR Spectrum of C_4 Complex

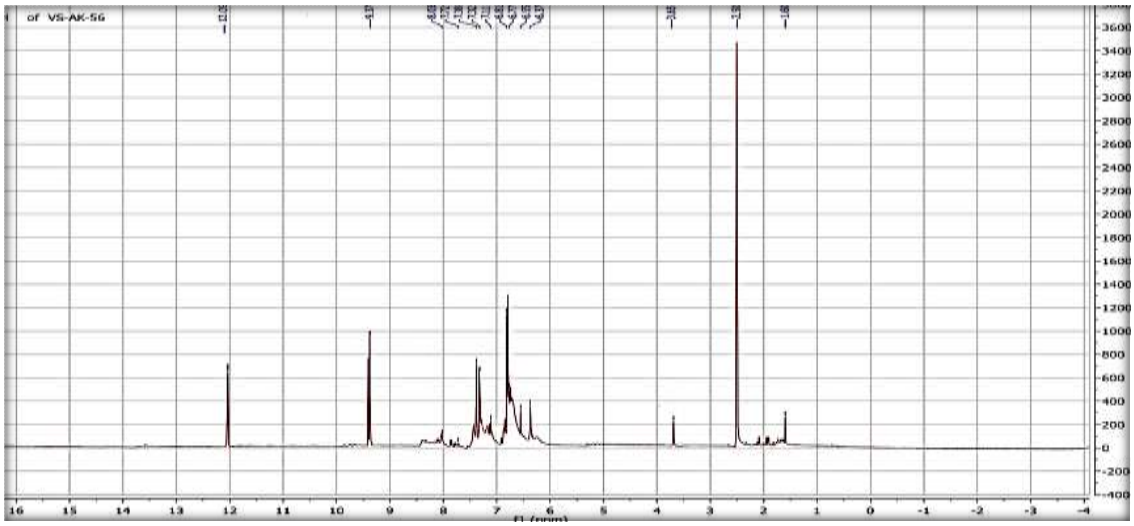

Figure 18: ^{1}H-NMR Spectrum of C_5 Complex

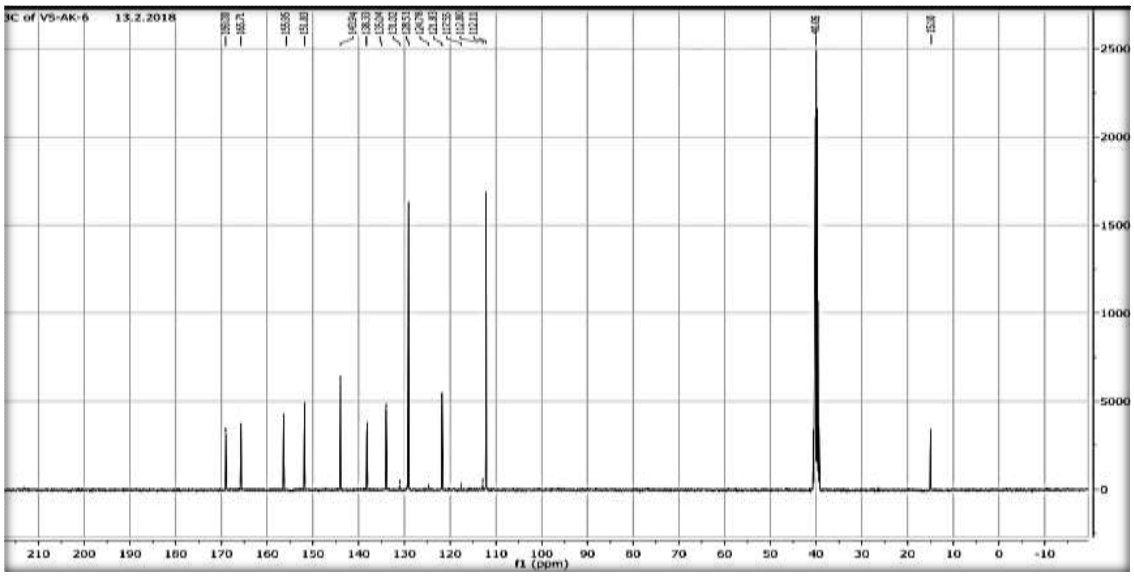

Figure 19: ^{13}C-NMR Spectrum of L

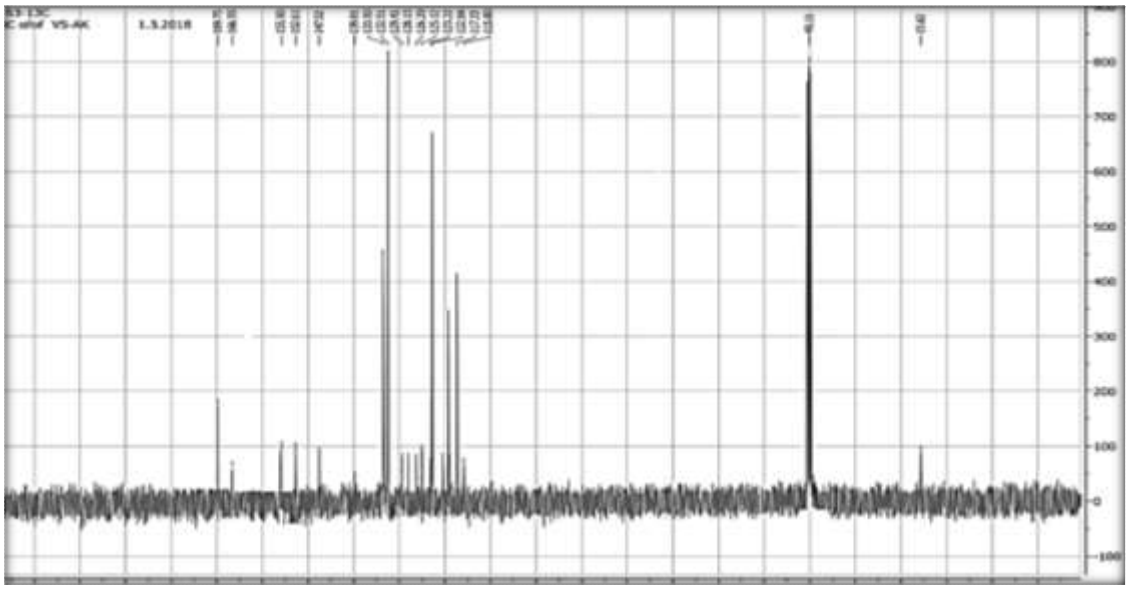

Figure 20: ^{13}C-NMR Spectrum of C_1 Complex

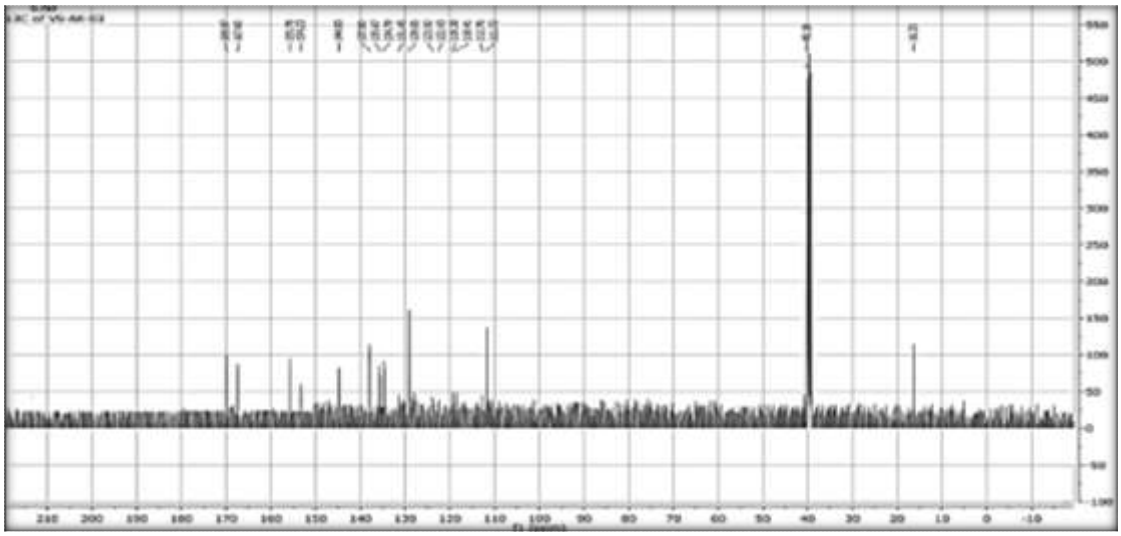

Figure 21: ^{13}C-NMR Spectrum of C_2 Complex

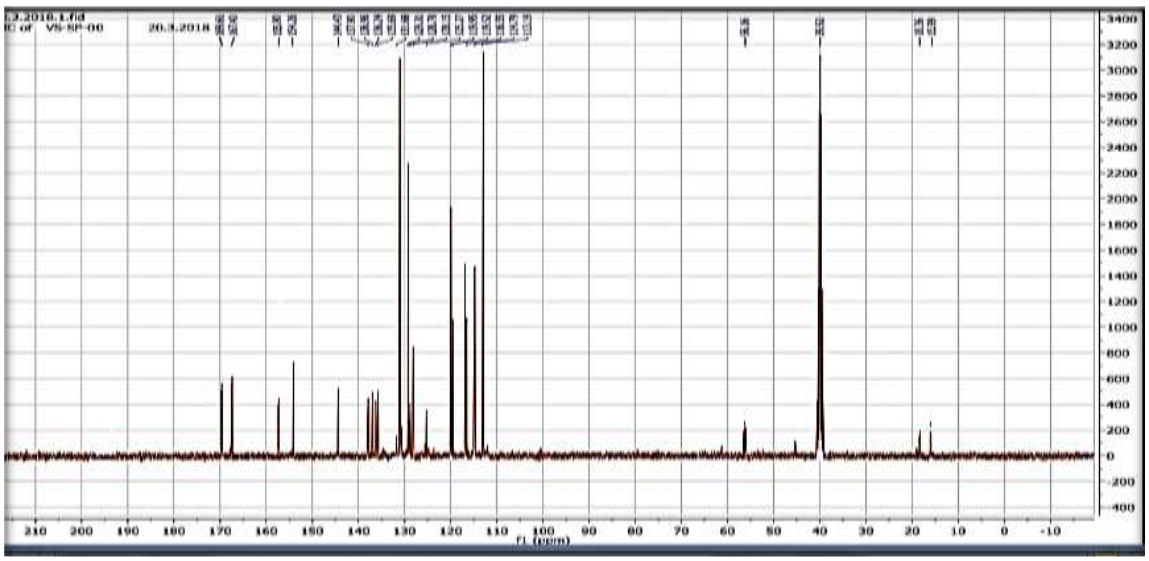

Figure 22: ^{13}C-NMR Spectrum of C_3 Complex

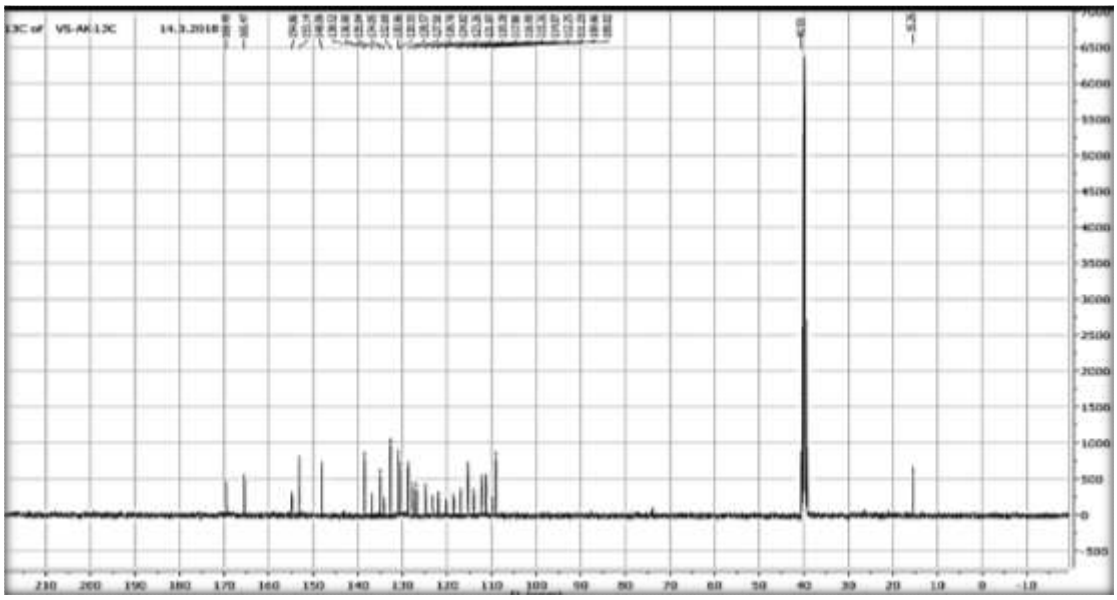

Figure 23: ^{13}C-NMR Spectrum of C_4 Complex

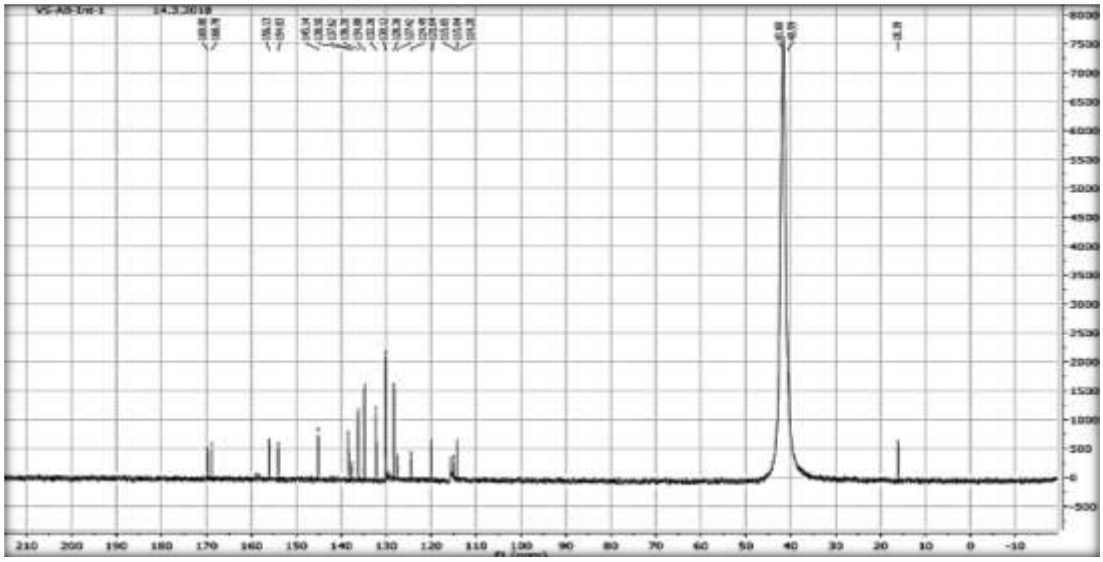

Figure 24: ^{13}C-NMR Spectrum of C_5 Complex

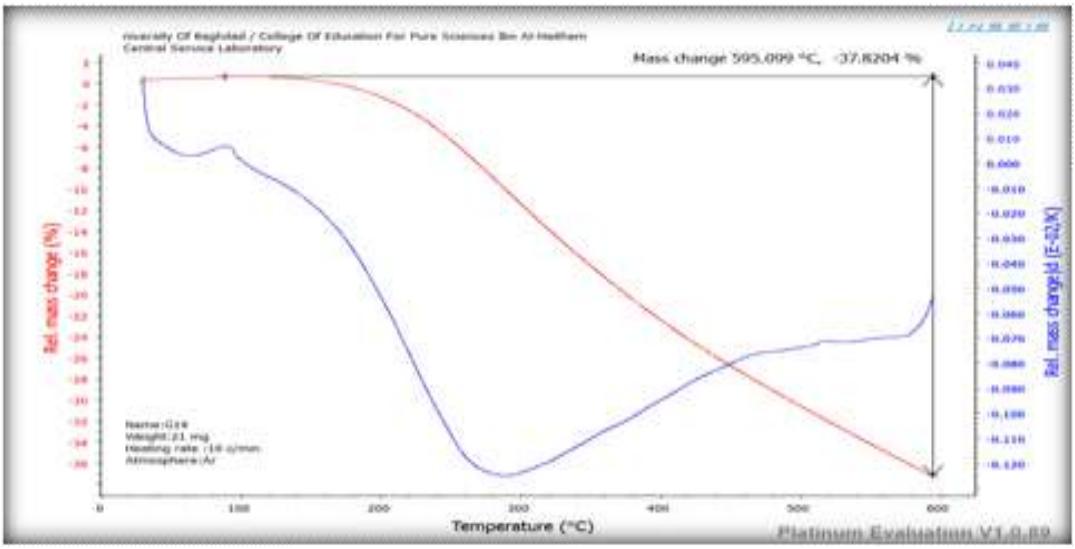

Figure 25: The thermogram of ligand (L)

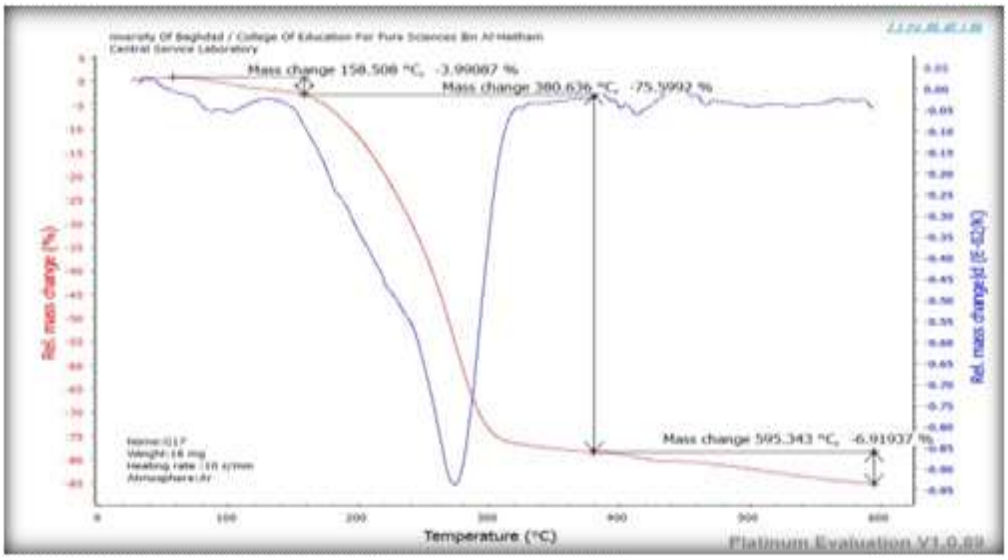

Figure 26: The thermogram of C_1 complex

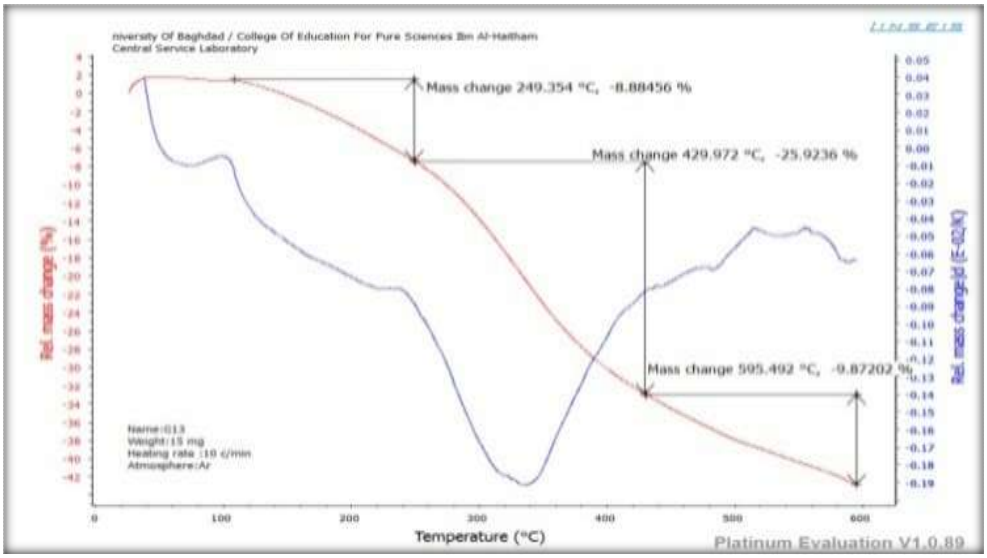

Figure 27: The thermogram of C_2 complex

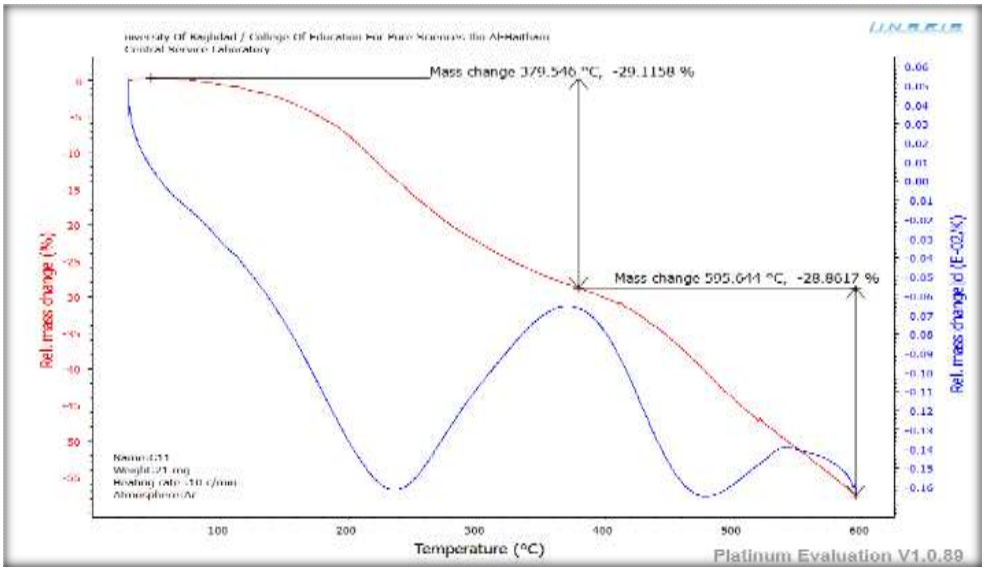

Figure 28: The thermogram of C_3 complex

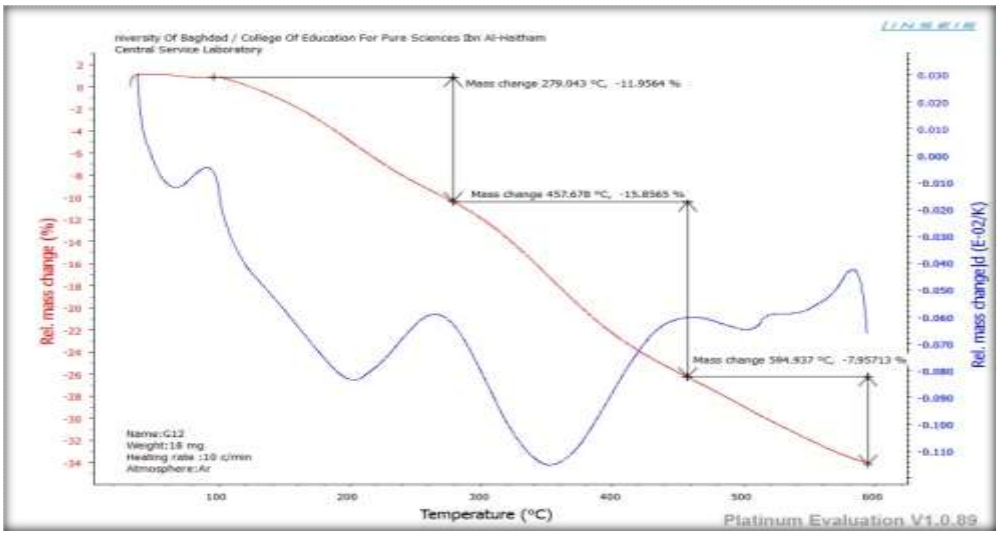

Figure 29: The thermogram of C_4 complex

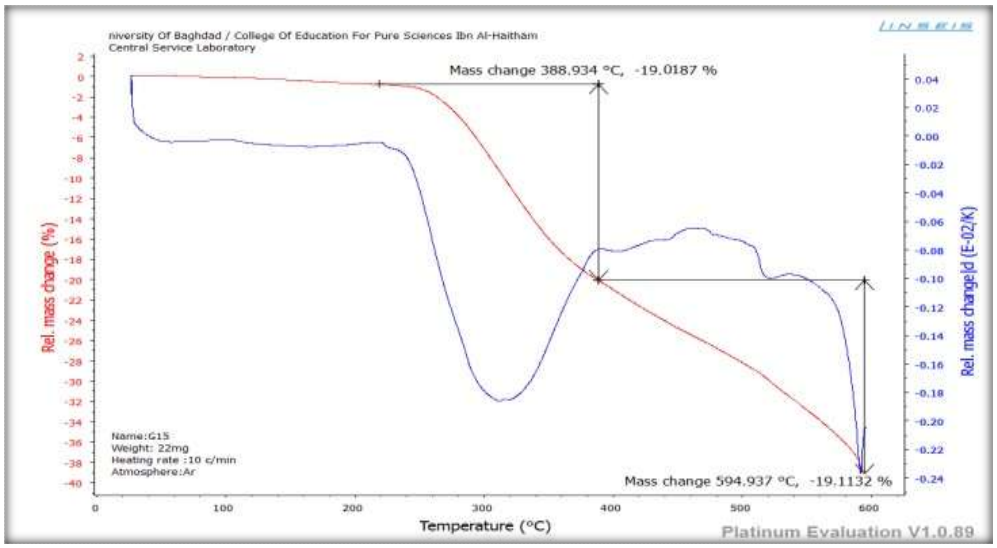

Figure 30: The thermogra of C_5 complex

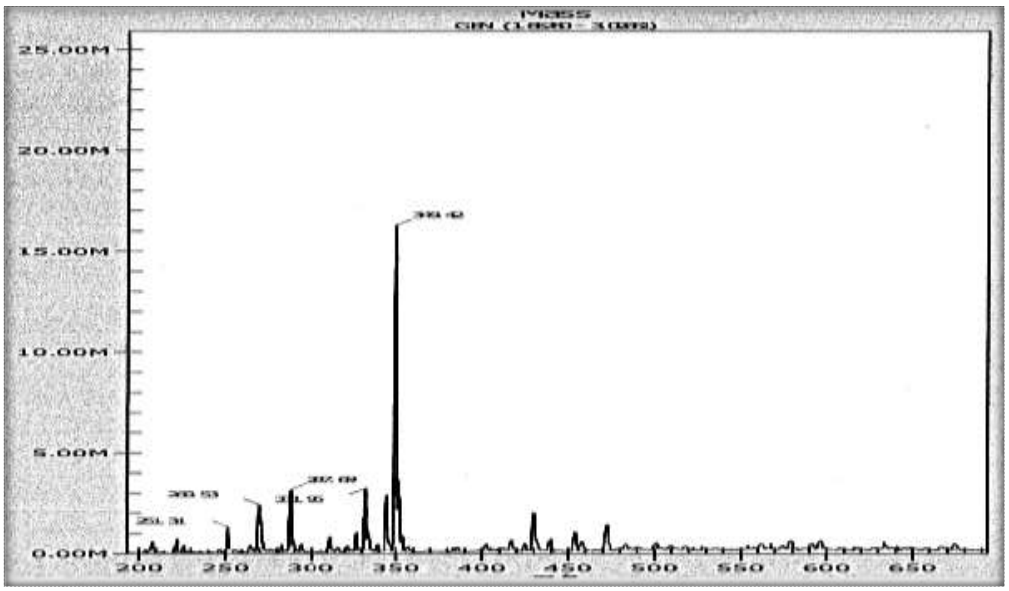

Figure 31: The spectram of ligand

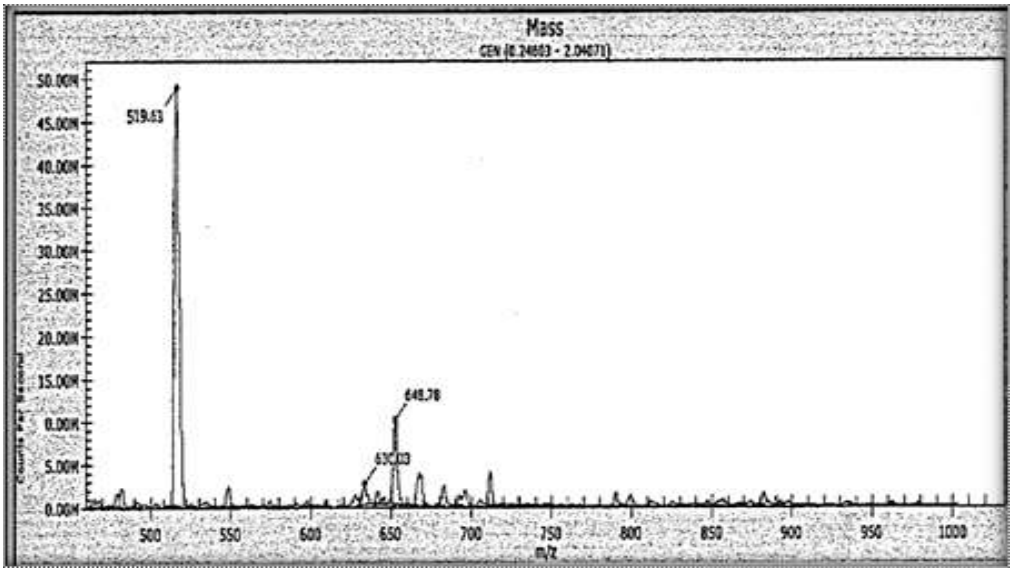

Figure 32: The spectram of comples (C_1)

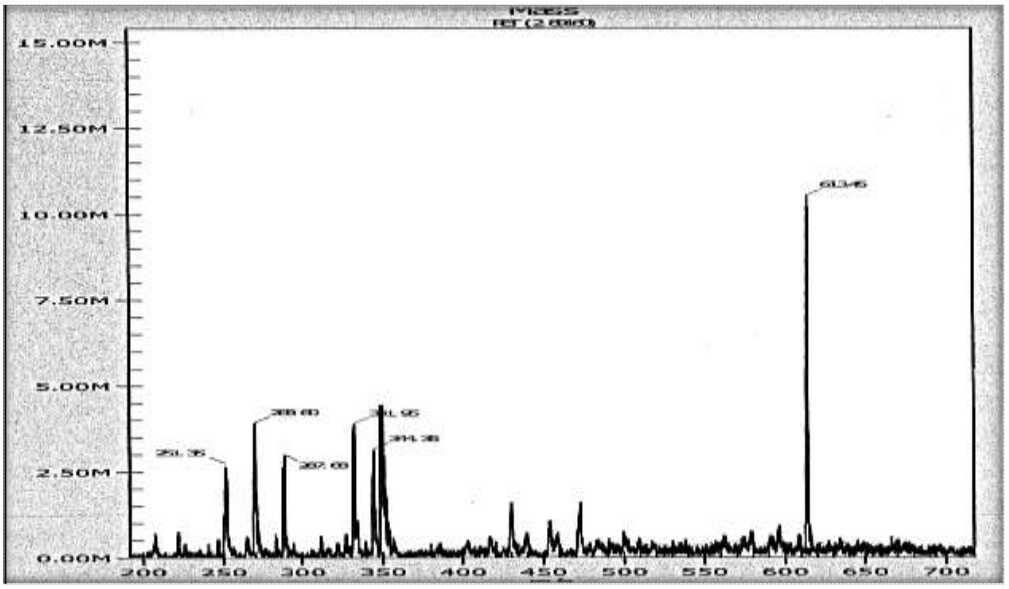

Figure 33: The spectram of comples (C_2)

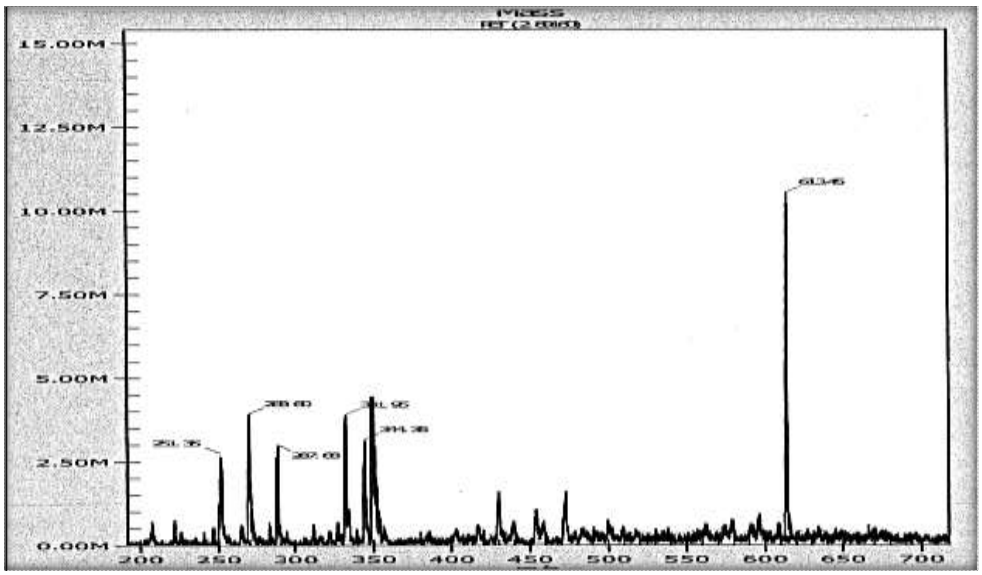

Figure 34: The spectram of comples (C_3)

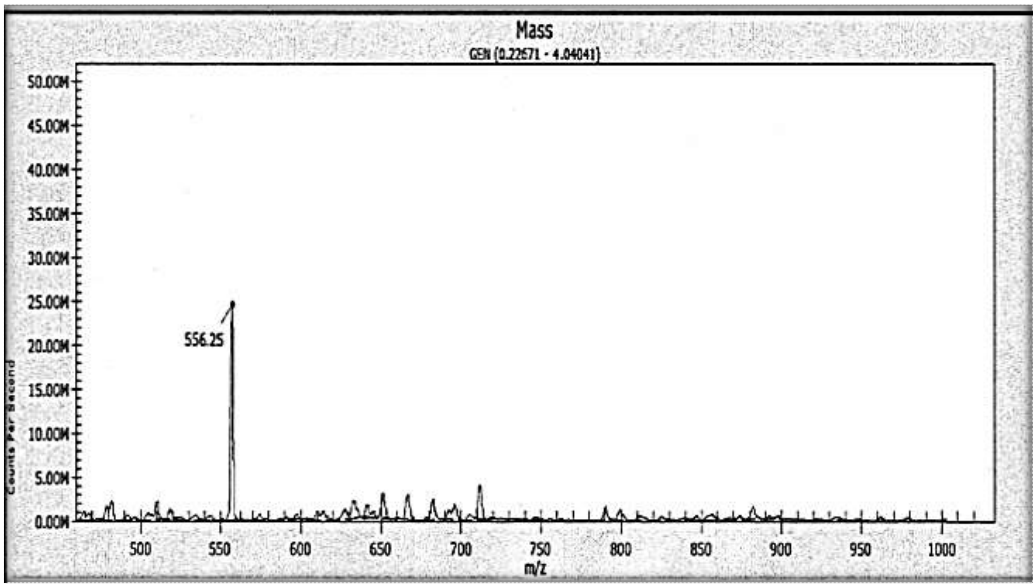

Figure 35: The spectram of comples (C_4)

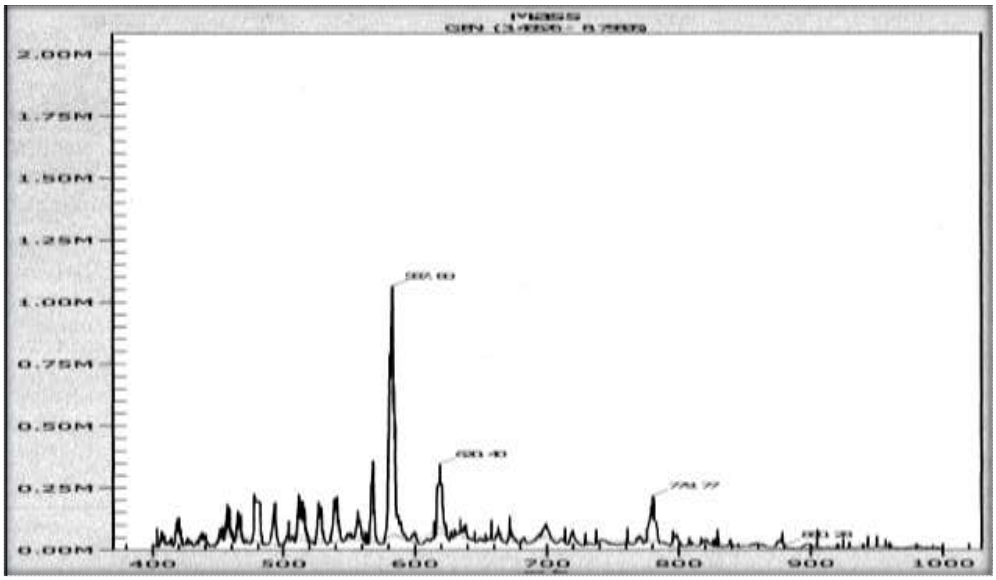

Figure 36: The spectram of comples (C_5)

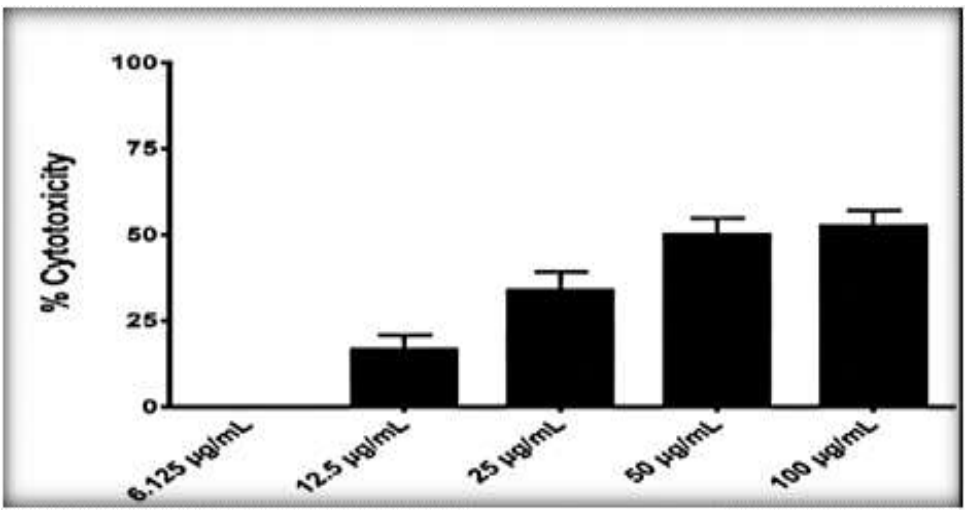

Figure 37: Cytotoxic effect of ligand (L) in AMJM

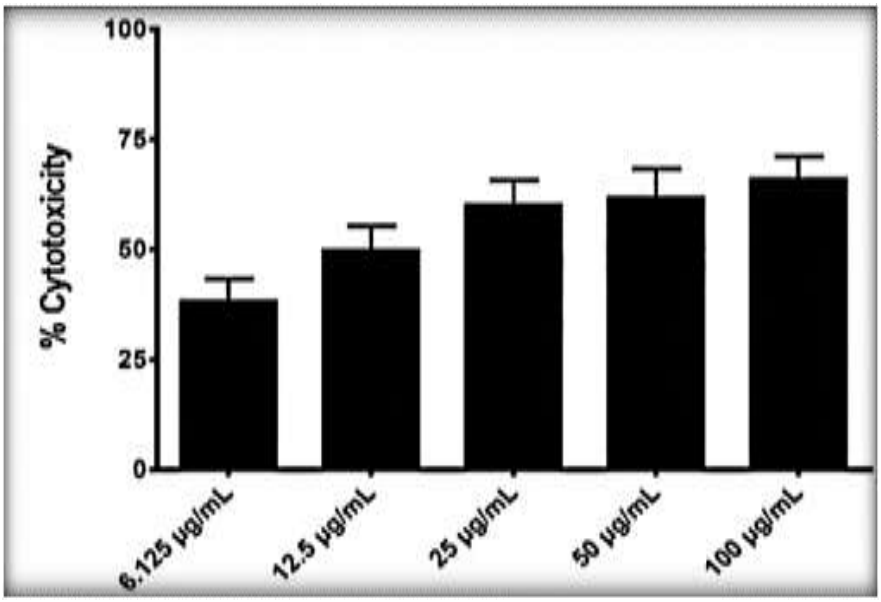

Figure 38: Cytotoxic effect of complex (C_1)

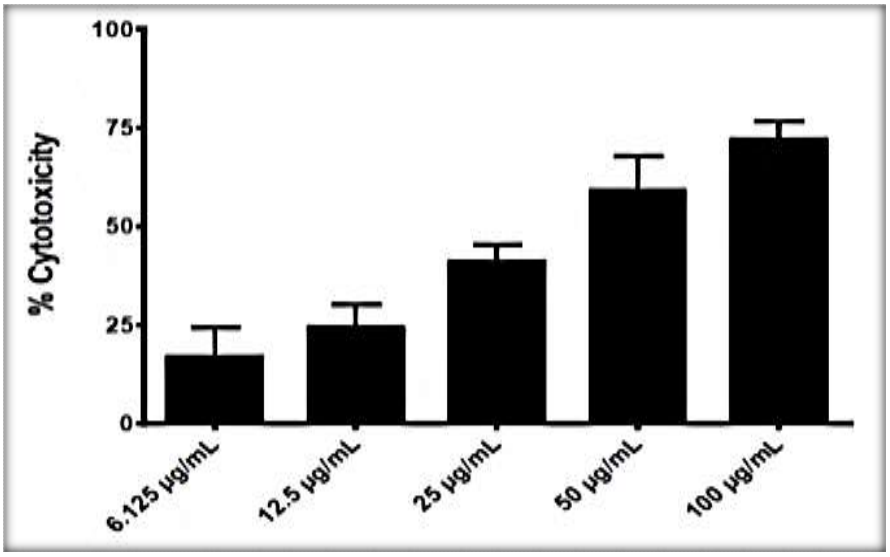

Figure 39: Cytotoxic effect of complex (C_2) in AMJM

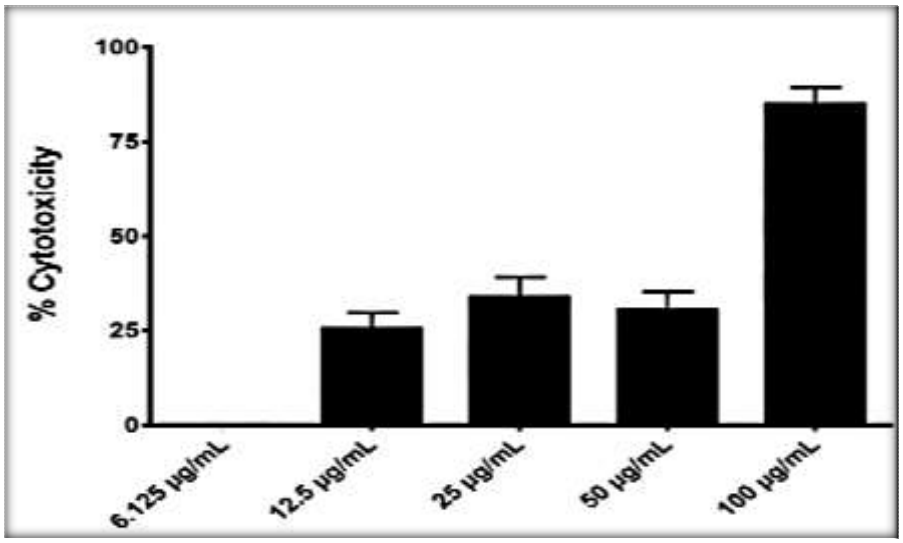

Figure 40: Cytotoxic effect of complex (C_3) in AMJM

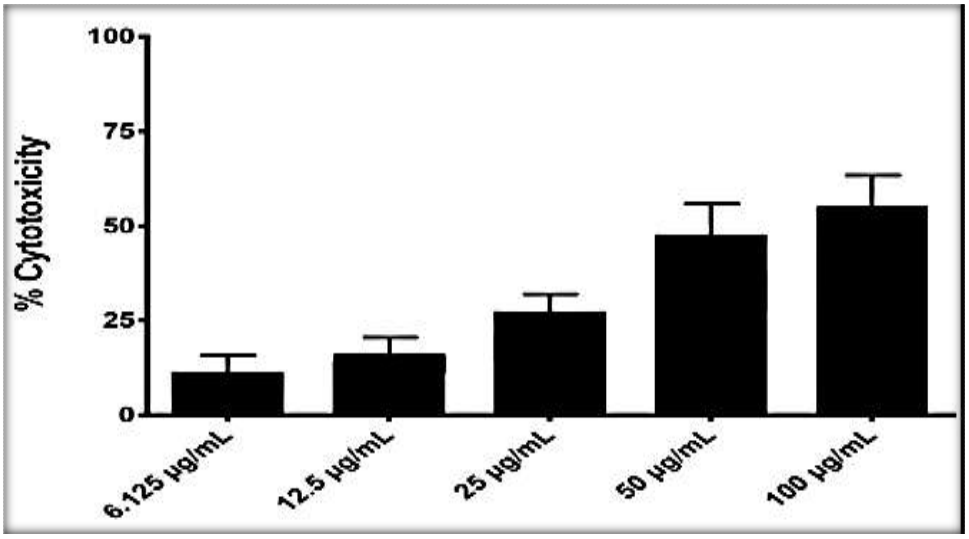

Figure 41: Cytotoxic effect of complex (C_4) in AMJM

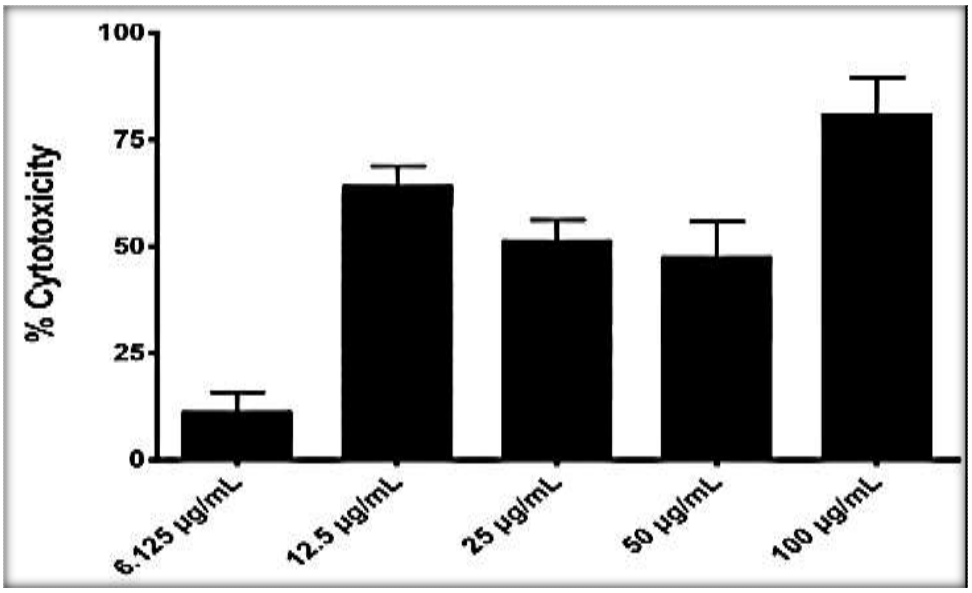

Figure 42: Cytotoxic effect of complex (C_5) in AMJM

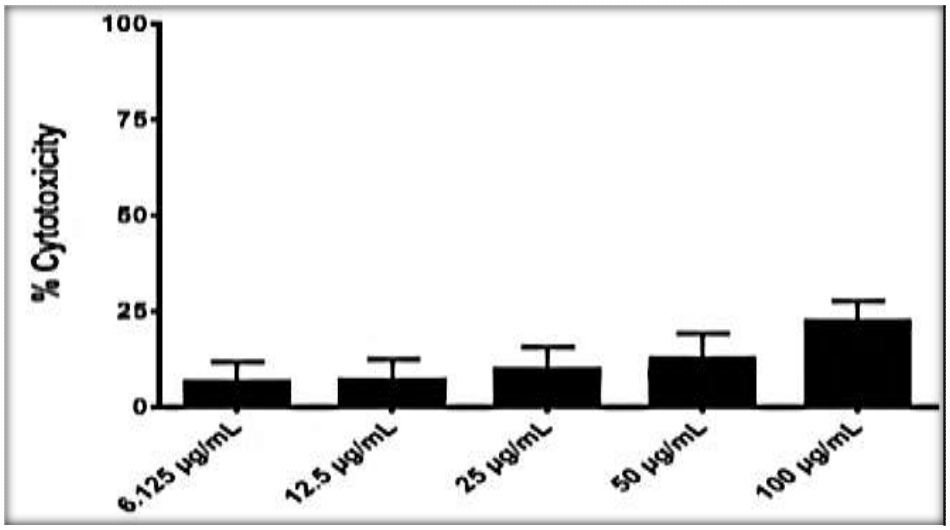

Figure 43: Cytotoxic effect of ligand (L_1) in HeLa

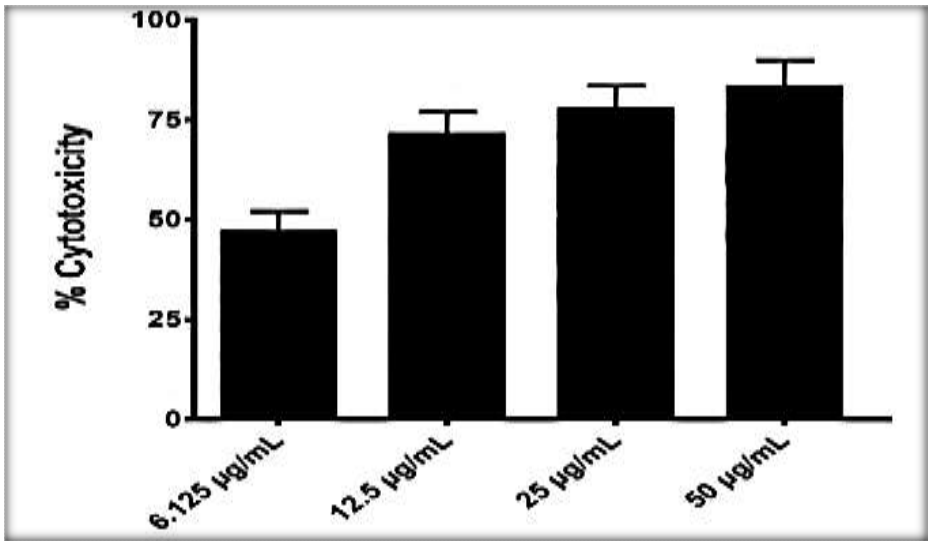

Figure 44: Cytotoxic effect of complex (C_1) in HeLa

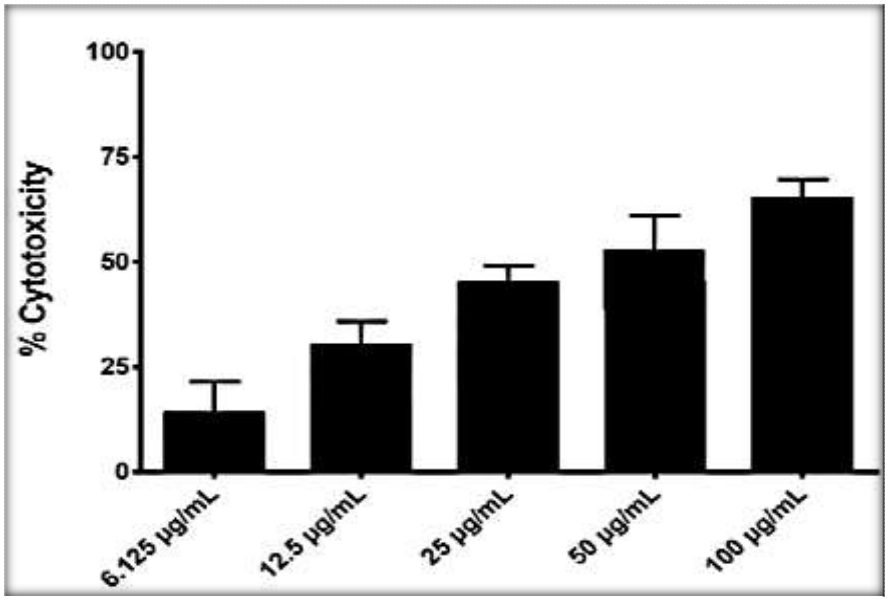

Figure 45: Cytotoxic effect of complex (C_2) in HeLa

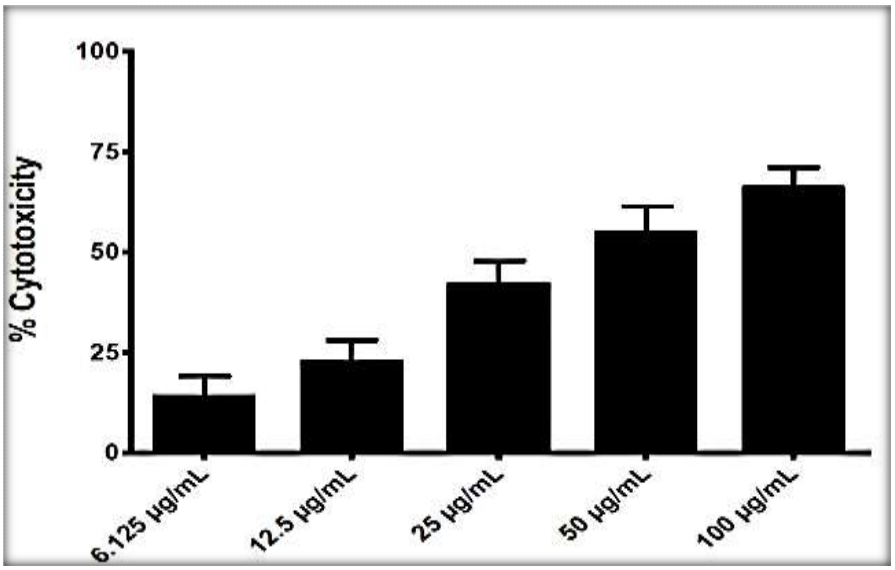

Figure 46: Cytotoxic effect of complex (C_3) in HeLa

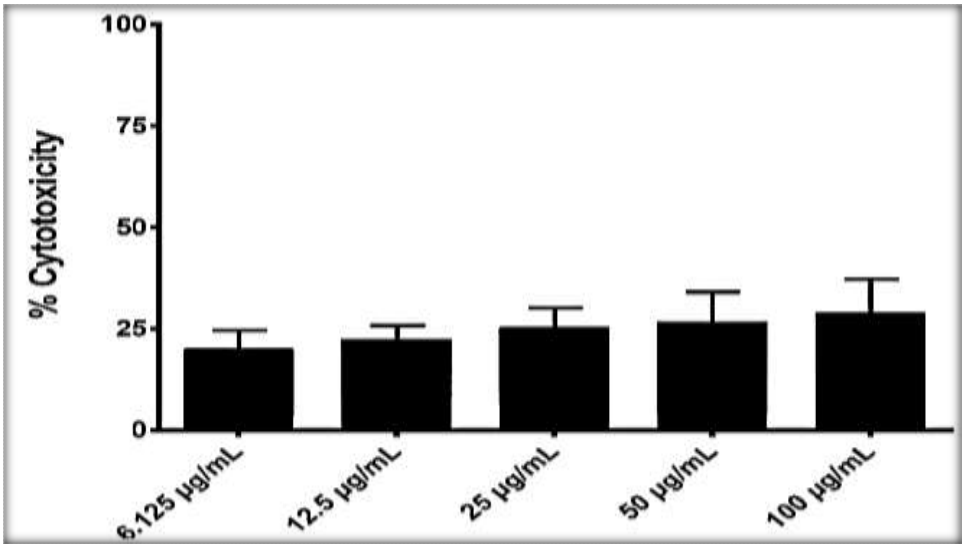

Figure 47: Cytotoxic effect of complex (C_4) in HeLa

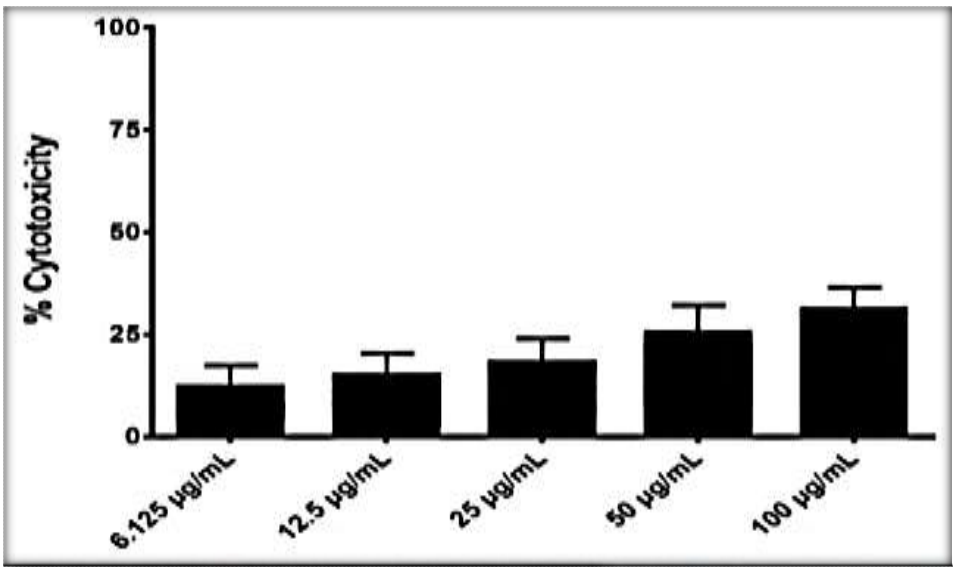

Figure 48: Cytotoxic effect of complex (C_5) in HeLa

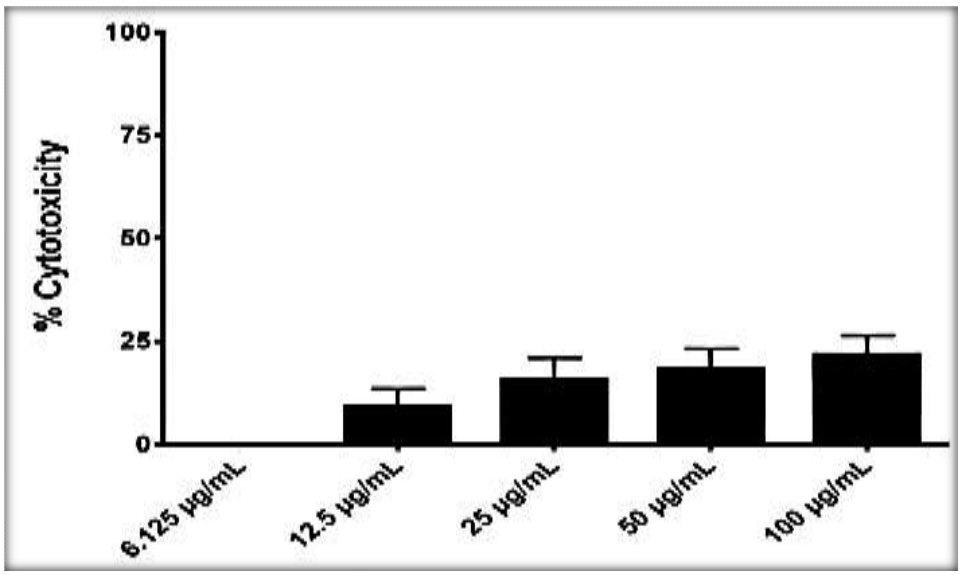

Figure 49: Cytotoxic effect of ligand (L_1) in SKOV-3

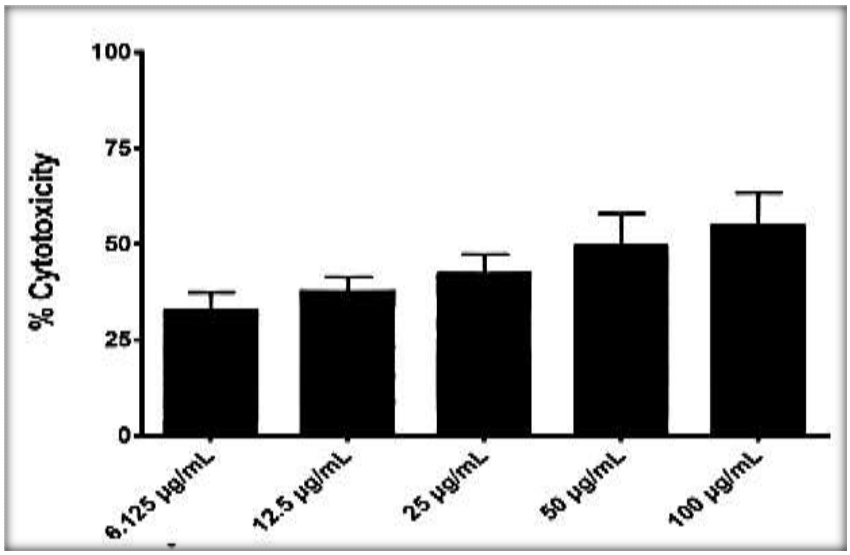

Figure 50: Cytotoxic effect of complex (C_1) in SKOV-3

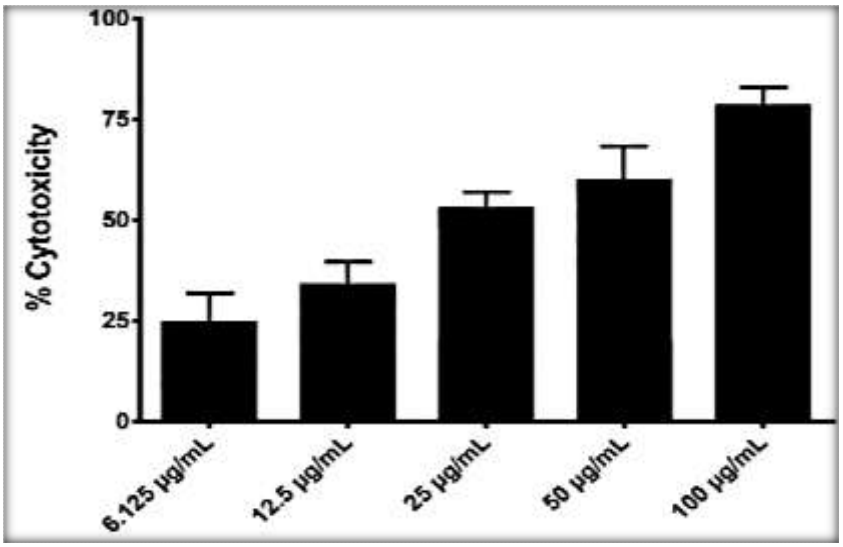

Figure 51: Cytotoxic effect of complex (C_2) in SKOV-3

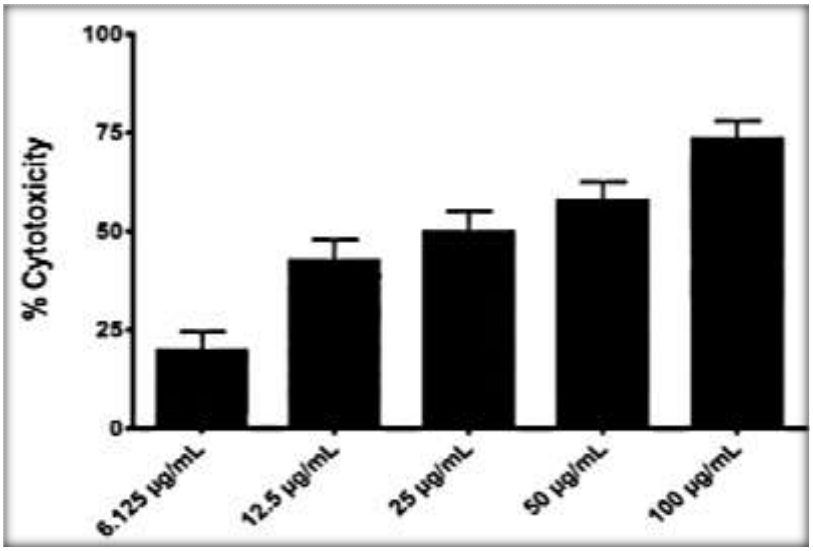

Figure 52: Cytotoxic effect of complex (C_3) in SKOV-3

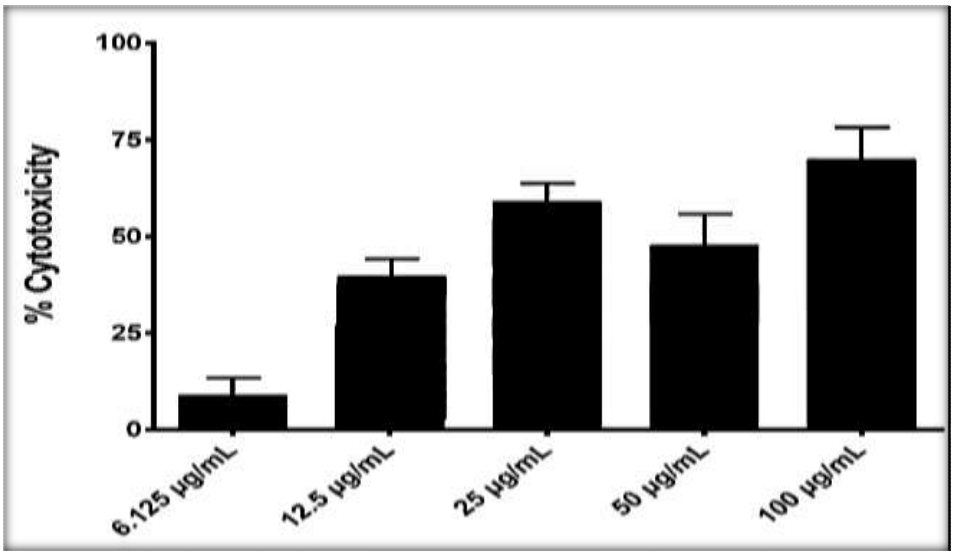

Figure 53: Cytotoxic effect of complex (C_4) in SKOV-3

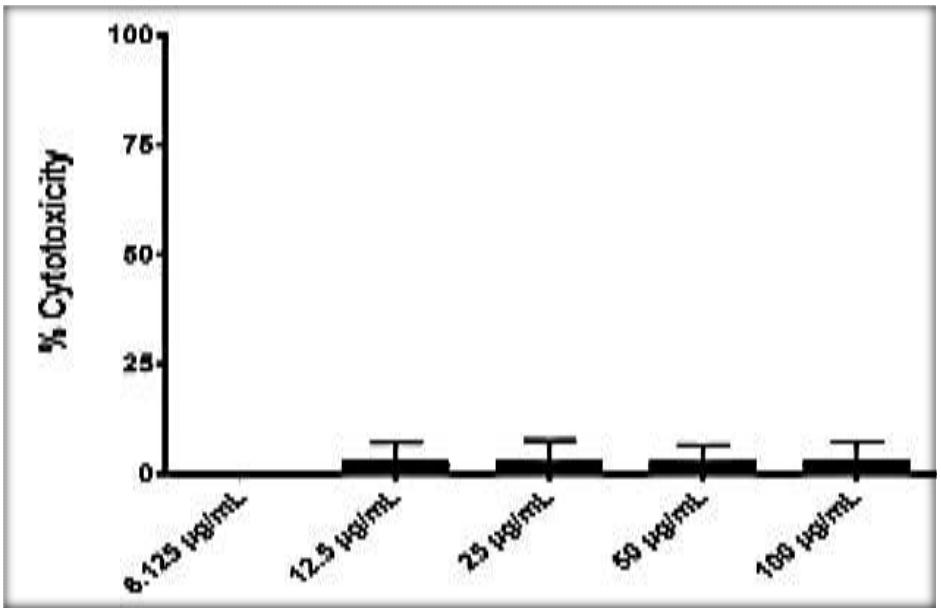

Figure 54: Cytotoxic effect of complex (C_5) in SKOV-3

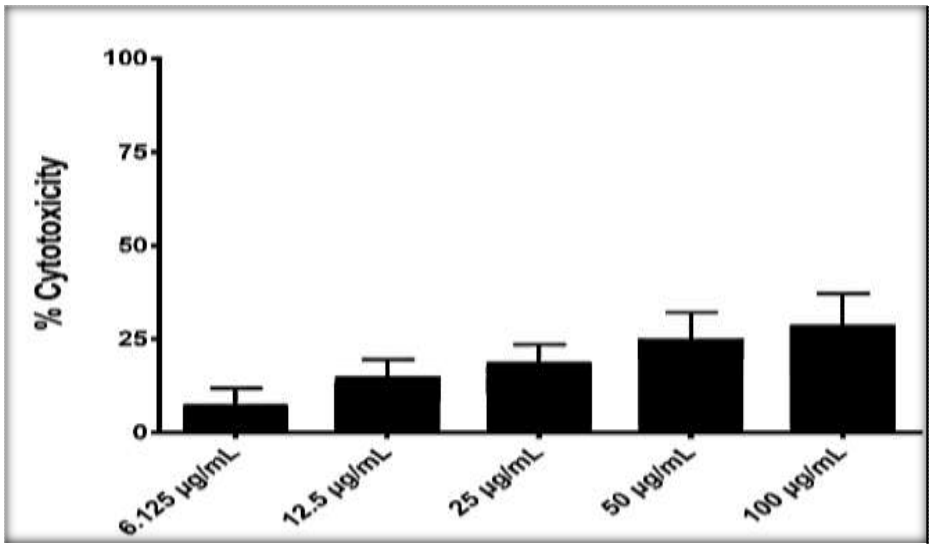

Figure 55: Cytotoxic effect of ligand (L) in CMF-7

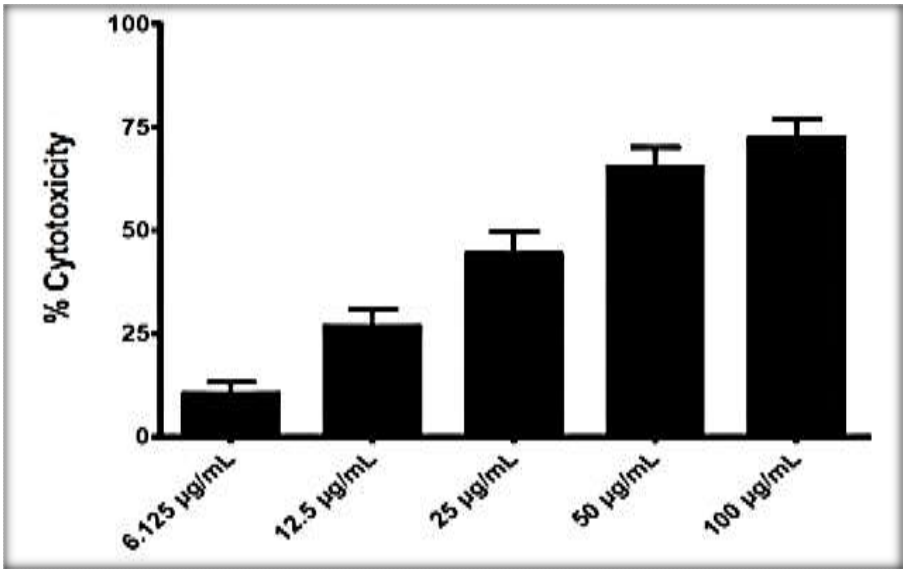

Figure 56: Cytotoxic effect of complex (C_1) in CMF-7

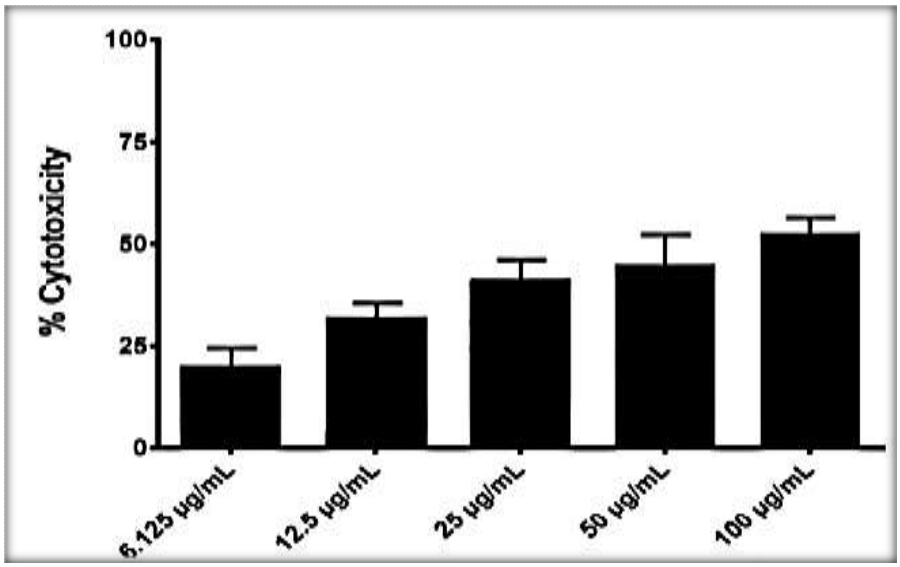

Figure 57: Cytotoxic effect of complex (C_2) in CMF-7

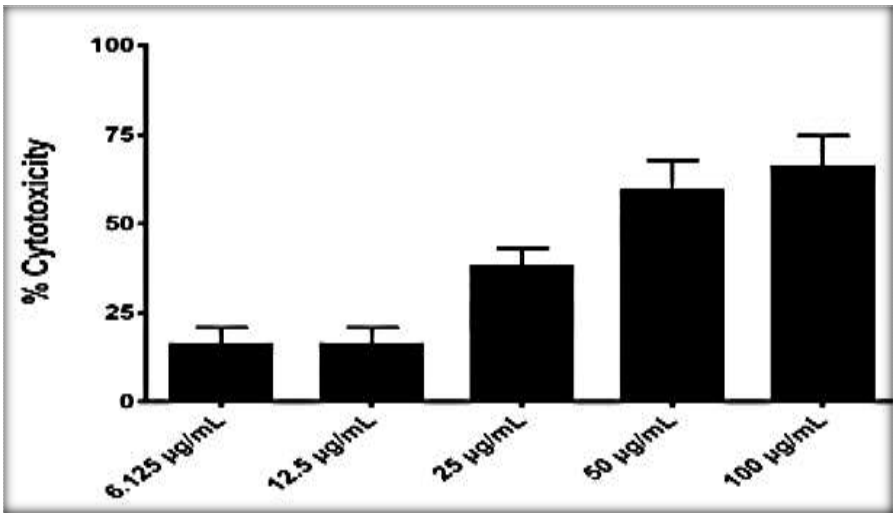

Figure 58: Cytotoxic effect of complex (C_3) in CMF-7

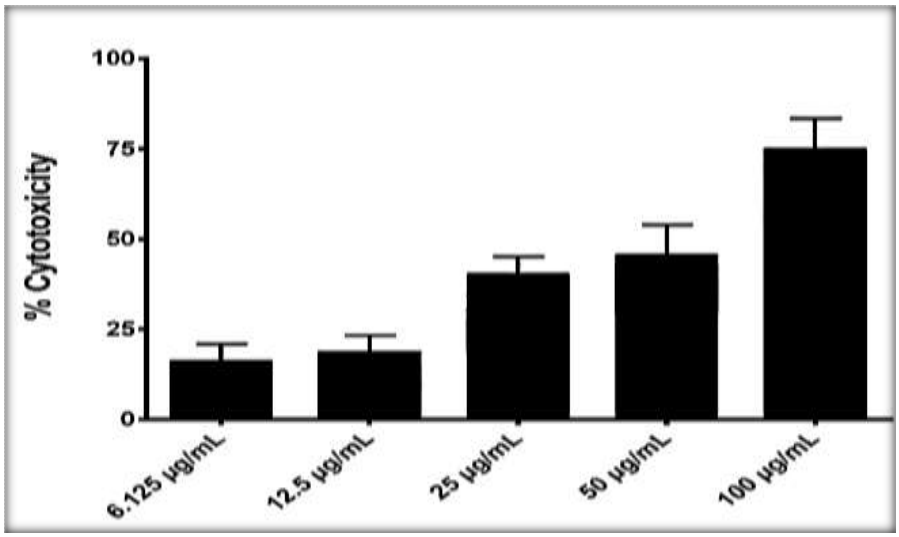

Figure 59: Cytotoxic effect of complex (C_4) in CMF-7

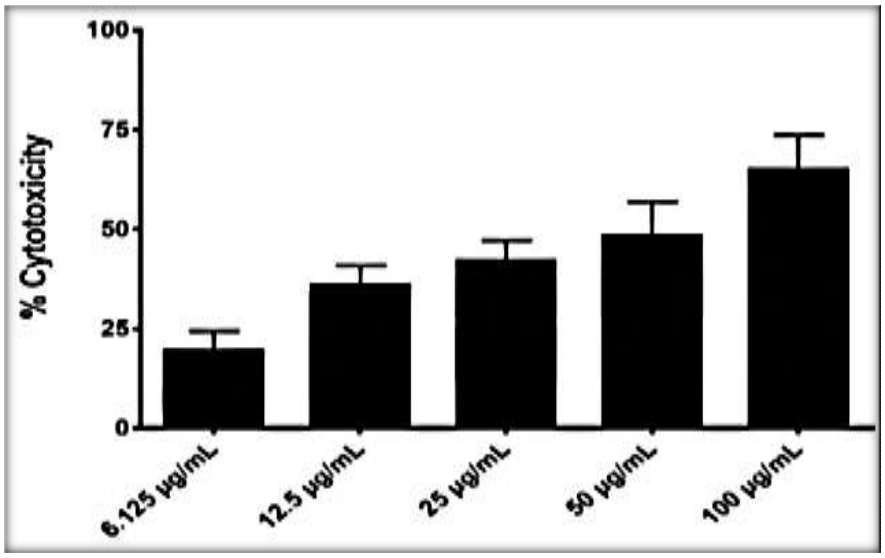

Figure 60: Cytotoxic effect of complex (C_5) in CMF-7

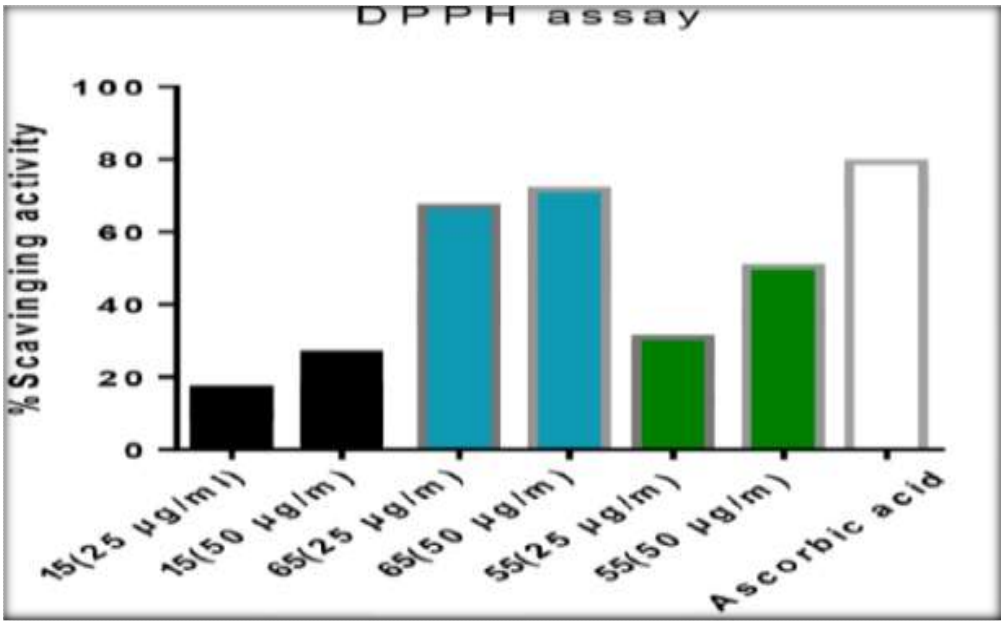

Figure 61: Scavenging activity of (L_1 Black color), (C_3 Blue color and (C_2 Green color)

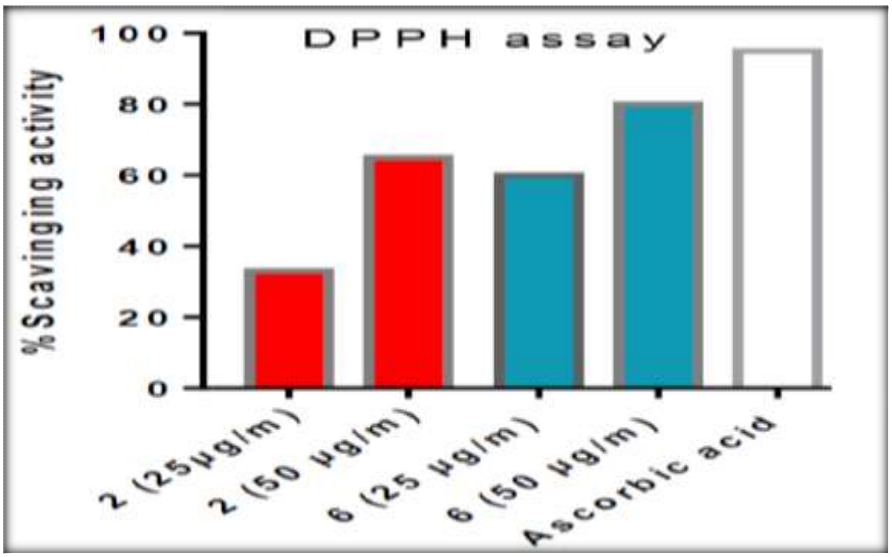

Figure 62: Scavenging activity of (C_4 Red color) and (C_1 Blue color)

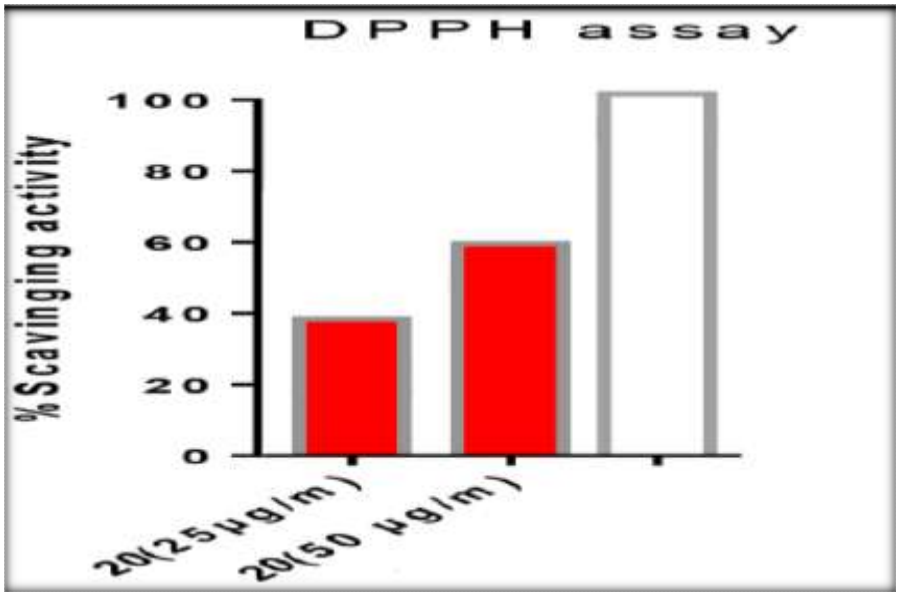

Figure 63: Scavenging activity of (C_5 Red color)

References

1. Schiff H., Mittheilungen aus dem Universitätslaboratorium in Pisa: eine neue Reihe organischer Basen, *Eur Jou*., **131(1)**, 118-119 **(1864)**

2. Xavier A. and Srividhya N., Synthesis and study of Schiff base ligands, *IOSR-J Appl Chem*, **7**, 6-15 **(2014)**

3. Samal S., Das R., Dey R. and Acharya S., Chelating resins VI: Chelating resins of formaldehyde condensed phenolic Schiff bases derived from 4, 4′-diaminodiphenyl ether with hydroxybenzaldehydes—synthesis, characterization and metal ion adsorption studies, *JAPS*, **77(5)**, 967-981 **(2000)**

4. Varsha G., Arun V., Robinson P., Sebastian M., Varghese D., Leeju P., Jayachandran V. and Yusuff P., Two new fluorescent heterocyclic perimidines: first syntheses, crystal structure and spectral characterization, *Tetrahedron Letters*, **51(16)**, 2174-2177 **(2010)**

5. Brewster C., Schiff's bases from 3, 5-dibromo-salicylaldehyde, *JACS*, **46(11)**, 2463-2468 **(1924)**

6. Roy Barman T., Sutradhar M., Drew M.G.B. and Rentschler E., 2-Amino-2-methyl-1,3-propanediol (ampdH2) as ligand backbone for the synthesis of cobalt complexes: Mononuclear Co(II), binuclear Co(II,III) and hexanuclear Co(II,III), *Polyhedron*, **51**, 192-200 **(2013)**

7. Suresh S., Bhuvanesh N., Prabhu J., Thamilselvan A., Kannan K. and Nandhakumar R., Pyrene based chalcone as a reversible fluorescent chemosensor for Al3+ ion and its biological applications, *JPPA*, **359**, 172-182 **(2018)**

8. Rogulski K.R., Freytag S.O., Zhang K., Gilbert J.D., Paielli D.L., Kim J.H., Heise C.C. and Kirn D.H., In vivo antitumor activity of ONYX-015 is influenced by p53 status and is augmented by radiotherapy, *Cancer Research*, **60(5)**, 1193-1196 **(2000)**

9. Al-Shammari A.M., Salman M.I., Saihood Y.D., Yaseen N.Y., Raed K., Shaker H.K., Ahmed A., Khalid A. and Duiach A., In vitro synergistic enhancement of Newcastle Disease Virus to 5-fluorouracil cytotoxicity against tumor cells, *Biomedicines*, **4(1)**, 202-209 **(2016)**

10. Raman N., Thalamuthu S., Dhaveethuraja J., Neelakandan M. and Banerjee S., DNA cleavage and antimicrobial activity studies on transition metal (II) complexes of 4-aminoantipyrine derivative, *JCCHEMS*, **53(1)**, 1439-1443 **(2008)**

11. Kubaisi A.A. and Ismail K.Z., Nickel (II) and palladium (II) chelates of dehydroacetic acid Schiff bases derived from thiosemicarbazide and hydrazinecarbodithioate, *Canadian Journal of Chemistry*, **72(8)**, 1785-1788 **(1994)**

12. Spinu C. and Kriza A., Co (II), Ni (II) and Cu (II) complexes of bidentate Schiff bases, *ACSI*, **47(2)**, 179-186 **(2000)**

13. Boghaei D.M. and Mohebi S., Non-symmetrical tetradentate vanadyl Schiff base complexes derived from 1,2-phenylene diamine and 1,3-naphthalene diamine as catalysts for the oxidation of cyclohexene, *Tetrahedron*, **58(26)**, 5357-5366 **(2002)**

14. Doadrio A.L., Sotelo J. and Fernández-Ruano A., Synthesis and characterization of oxovanadium (IV) dithiocarbamates with pyridine, *Quim. Nova*, **25(4)**, 525-528 **(2002)**

15. Rasheed R.T., Synthesis of new metal complexes derived from 5-nitroso 8-hydroxy quinoline and Salicylidene P-imino acetophenone with Fe (II), Co (II), Ni (II) and Cu (II) ions, *JNUS*, **15(4)**, 68-73 **(2012)**

16. Ansari R.M. and Bhat B.R., Schiff base transition metal complexes for Suzuki–Miyaura cross-coupling reaction, *Journal of Chemical Sciences*, **129(9)**, 1483-1490 **(2017)**

17. Abdel-Rahman L., Abudief A., Moustafa H. and Hamdan S., Ni(II) and Cu(II) complexes supported by ONNO asymmetrical tetradentate Schiff base ligand: Synthesis, spectroscopic characterization, theoretical calculations, DNA interaction and antimicrobial studies, *Applied Organometallic Chemistry*, **31(2)**, 1-12 **(2016)**

18. Caro A.A. et al, Prooxidant and antioxidant properties of salicylaldehyde isonicotinoyl hydrazone iron chelators in HepG2 cells, *Biochim Biophys Acta*, **1850(11)**, 2256-2264 **(2015)**

19. Gottlieb H.E., Kotlyar V. and Nudelman A., NMR chemical shifts of common laboratory solvents as trace impurities, *JOC*, **62(21)**, 7512-7515 **(1997)**

20. Ghorab M.M., Ragab F.A., Heiba H.I. and Soliman A.M., Anticancer and radio-sensitizing evaluation of some new sulfonamide derivatives bearing pyridone, thiophene and hydrazone moieties, *Research on Chemical Intermediates*, **43(8)**, 4657-4681 **(2017)**

21. Abdel-Aziz M., Park S.E., Abuo-Rahma G.E.D.A., Sayed M.A. and Kwon Y., Novel N-4-piperazinyl-ciprofloxacin-chalcone hybrids: synthesis, physicochemical properties, anticancer and topoisomerase I and II inhibitory activity, *EJMC*, **69**, 427-438 **(2013)**

22. Sun R.W.Y., Ma D.L., Wong E.L.M. and Che C.M., Some uses of transition metal complexes as anti-cancer and anti-HIV agents, *Dalton Transactions*, **43**, 4884-4892 **(2007)**.

****